Youngstown State University

William Rayen School of Engineering

A SOLID STATE CONVERTER FOR MEASUREMENT OF AIRCRAFT NOISE AND SONIC BOOM

Final Report of Research Performed under NASA Grant NGR 36-028-004

submitted to the

National Aeronautics and Space Administration

Principal Investigator: Allan J. Zuckerwar
Assistant Professor
Electrical Engineering

Personnel: William Wheeler Shope
Graduate Research Assistant

Period: September 1, 1971 to August 31, 1972

Date of Submission: November 30, 1972

Youngstown State University

William Rayen School of Engineering

A SOLID STATE CONVERTER FOR MEASUREMENT OF AIRCRAFT NOISE AND SONIC BOOM

Final Report of Research Performed under NASA Grant NGR 36-028-004

submitted to the

National Aeronautics and Space Administration

Principal Investigator: Allan J. Zuckerwar
Assistant Professor
Electrical Engineering

Personnel: William Wheeler Shope
Graduate Research Assistant

Period: September 1, 1971 to August 31, 1972

Date of Submission: November 30, 1972

I. OBJECTIVE

The objective of the research performed under NASA Grant NGR 36-028-004 is to develop a solid state converter for use in a system of instrumentation for measuring aircraft noise and sonic boom. The research program encompasses all aspects of the development of the system: theoretical analysis, practical design and construction of a prototype converter, and testing in both the laboratory and the field. It is intended that the converter, used in conjunction with a "zero drive" amplifier of MB Electronics, Inc., will serve the dual purpose of

a) alleviating many of the problems encountered in present systems, such as limited frequency response, expensive connecting cables, sensitivity to cable length and type, and high sensitivity to environmental conditions (ambient temperature and humidity), and

b) providing a single system to cover a wide range of applications presently undertaken with a variety of systems.

The following specification have been set forth for the system under development:

a) Frequency response: 0.02 Hz to 20 kHz.

b) Dynamic range: 70 dB in two steps

   (1) 60-130 for aircraft noise and

   (2) 90-160 for sonic boom.

c) Insensitivity to cable length and type.

d) Insensitivity to ambient temperature and humidity.

II. DESCRIPTION OF THE SYSTEM

Figure 1 shows a block diagram of the system. The converter produces an electrical current proportional to the sound pressure level (SPL) at the condenser microphone. The signal is transmitted over a cable typically 1800' in length, amplified by the Model N400 Zero Drive Amplifier of MB Electronics, Inc., and recorded on magnetic tape.

The converter circuit has evolved from a modified form of what was once known as the Widdington Micrometer, described by Alexander [1]. His circuit contains but a single active element -- a multi-electrode vacuum tube, an octode -- and is based on the principle of the pentagrid converter, a circuit which finds extensive application in the field of commercial broadcasting. Especially favorable are its characteristics with regard to conversion gain, frequency response, dynamic range, input impedance, and operational simplicity. In the converter developed under this grant the pentagrid converter circuit is adapted specifically for the purpose of measuring the displacements of the diaphram in a condenser microphone, whereby the octode is replaced by a dual-gate field-effect transistor (Texas Instruments Type 3N202 n-channel MOSFET), and the output stage is designed for compatability with the zero drive amplifier.

A circuit diagram of two prototype converters delivered to NASA-Langley Research Center is shown in Fig. 2. The circuit components are housed in a brass tube, approximately three inches long and one inch in diameter. One end of the tube screws into a Bruel & Kjaer Type UA0300 Input Adapter, and the other end contains a standard BNC female connector to the cable. A Type 4133 1/2" microphone cartridge screws into the other end of the UA0300.

Transistor T_1 and quartz crystal X make up the core of a local oscillator, which drives gate 2 (G_2) of the field-effect transistor F at 9.008 MHz. A tank circuit, consisting of the condenser microphone C and inductor L is connected to gate 1 (G_1) and tuned to the carrier frequency. As a result of drain-to-gate capacitive coupling a small fraction of the drain current leaks into the tank circuit and produces a voltage at gate 1. Now because the transconductance with respect to gate 1 -- that is, the ratio of drain current to voltage at gate 1 -- is extremely sensitive to the voltage applied at gate 2, the signal at gate 1 mixes with that at gate 2 to generate a direct drain current component (over and above the quiescent current). A change in the capacitance C changes the level of this direct current; consequently a periodic change in C, as caused by the presence of sound at the microphone, produces a periodic FET current at the frequency of the sound. The drain-to-gate capacitive coupling is an unwanted effect when the FET is used in a conventional mixer circuit, but here the effect is used to advantage and renders possible the detection of very small changes in the capacitance C. Transistor T_2 provides some voltage gain and capacitor C_4 filters out the carrier. The Darlington Amplifier T_3 is connected in a common collector configuration to better match the high output impedance of Transistor T_2 to the extremely low input impedance of the N400 zero drive amplifier.

In one of the prototype converters (Converter 1) the tank circuit is tuned by varying the inductor L. For this unit the inductor is located inside the brass tube and the UA0300 remains in tact. In the second prototype (Converter 2) a trim capacitor is connected in parallel with the microphone to tune the tank circuit. Here the UA0300 is modified in two ways: first, the guard ring is removed in order to reduce the capacitance in parallel with the microphone; secondly, the case is machined to seat the inductor and

trim capacitor. Converter 2 has a higher conversion gain (output current per unit SPL) than Converter 1, because the fixed inductor of the former (with a toroidal core) has a much higher Q than the variable inductor of the latter, as will be discussed later.

The function of the N400 zero drive amplifier is twofold:

1) to provide a constant 22 volts at the converter terminals A-B, and

2) to amplify the converter signal for recording on magnetic tape.

The advantages of the zero drive system are amply discussed in literature available from the manufacturer [2]; in short these include insensitivity to cable length and type, and low triboelectric and other types of noise. Normally an intermediate device, a "line driver," is connected between the signal source and zero drive amplifier. By eliminating the line driver we are able to use the 22 volts on the line as the supply voltage for the converter without undermining the performance of the zero drive amplifier.

A problem arises in system grounding when we connect the converter directly to the zero drive amplifier. The converter ground is negative with respect to the supply voltage, the zero drive ground positive. Consequently it is necessary to reverse the leads of the input connector of the zero drive amplifier; as a result, the converter housing, which is grounded, lies 22 volts below the signal ground of the amplifier, and the cable shield is by necessity left floating.

An attempt was made to relieve the grounding problem by redesigning the converter with a p-channel dual-gate junction FET (Siliconex type 3N89, the only such type available) and npn transistors, and accordingly reversing the converter polarity. However, because the redesigned converter showed a much lower conversion gain than the original, the attempt was abandoned.

III. THEORETICAL ANALYSIS OF THE CONVERTER CIRCUIT

A. Circuit Model and Transfer Function

In the circuit of Fig. 2 gate 1 has zero bias voltage, as this is unnecessary for class A operation of the FET. Gate 2, on the other hand, is biased at +2 V, about which the local oscillator output, having a peak-to-peak swing of ±2 V at 9.008 MHz, is superimposed. The corresponding variation in the gate 1 transconductance extends from 1-12.5 mmho. A greater swing in the gate 2 voltage does not bring a significantly greater variation in the gate 1 transconductance, as may be seen from Fig. 6. The supply voltage for the FET is essentially the Zener voltage of the Zener diode Z, namely 10 V, and the 330 Ω resistor for all practical purposes serves as the load.

The following symbols will appear in the analysis of the converter:

C_o = instantaneous microphone capacitance

C = static microphone capacitance

L = inductance in tank circuit

$\omega_o = 1/\sqrt{LC_o}$ = instantaneous resonant angular frequency of tank circuit

$\omega = 1/\sqrt{LC}$ = resonant angular frequency of tank circuit in absence of sound

= angular frequency of voltage driving gate 2

Q = quality factor of tank circuit

C_{gd} = gate 1-to-drain capacitance

g_{m1} = total gate 1 transconductance

a_o = gate 1 dc transconductance

a_1 = gate 1 "conversion" transconductance [3]

g_{m2} = gate 2 transconductance

r_d = drain resistance of FET

$v_2 = E_2 \cos\omega t$ = voltage driving gate 2

R_L = load resistance connected to drain.

Furthermore we adopt the following notation:

i, v = instantaneous values of current and voltage

$\bar{I}$, $\bar{V}$, $\bar{Z}_1$ = phasor representations,

I, V, Z_1 = phasor magnitudes.

The analysis is based upon the circuit model of the FET shown in Fig. 3. The gate-to-source capacitance is lumped with the microphone capacitance, and the drain-to-source capacitance is negligible because of the low load resistance. Here Z_1 is the impedance of the tank circuit:

$$Z_1 = \frac{j\omega L}{(1 - \omega^2/\omega_o^2) - j\omega/\omega_o Q} . \tag{1}$$

The behavior of the circuit is described by the following circuit equations:

$$g_{m1}v_1 + g_{m2}v_2 + i_1 + i_2 + i_d = 0 \tag{2}$$

$$I_1 = \bar{V}_1/\bar{Z}_1 \tag{3}$$

$$i_d = v_d/R_L \tag{4}$$

$$\bar{I}_1 = j\omega C_{gd}(\bar{V}_d - \bar{V}_1) \tag{5}$$

$$i_2 = (R_L/r_d)i_d . \tag{6}$$

From equations (3) and (5) we obtain a relationship between $\bar{V}_d$ and $\bar{V}_1$:

$$\bar{V}_1 = \frac{j\omega C_{gd}\bar{Z}_1\bar{V}_d}{1 + j\omega C_{gd}\bar{Z}_1} , \tag{7}$$

an equation which holds for each frequency component of $\bar{V}_1$ and $\bar{V}_d$.

We now follow an approach similar to that used in the analysis of the pentagrid converter [3]. We expand g_{m1} and the voltages in their Fourier series:

$$v_2 = E_2 \cos\omega t \tag{8}$$

$$g_{m1} = g_{m1}(v_2) = a_o + a_1 \cos\omega t + a_2 \cos 2\omega t + \ldots \tag{9}$$

$$v_1 = V_{11} \cos(\omega t + \phi) + \ldots \tag{10}$$

$$v_d = V_{do} + V_{d1} \cos(\omega t + \psi) \ldots \tag{11}$$

If the tank circuit has a high Q, then the impedance $\overline{Z}_1$ will be so large that

$$1/Z_1 << g_{m1}$$

and consequently

$$|i_1| << |i_d|$$

Thus we are justified in neglecting i_1 in Eq. (2).

Substitute the expressions (4), (6), and (8)-(11) into the remaining terms in Eq. (2) and gather coefficients of like functions of time. The DC terms[1] yield

$$V_{do} = -(1/2)\, a_1\, V_{11} \cos\phi\, R_L'. \tag{12}$$

In Eq. (12) is introduced R_L', the parallel combination of r_d and R_L:

$$1/R_L' = 1/r_d + 1/R_L . \tag{13}$$

The terms in $\cos\omega t$ and $\sin\omega t$ yield the following relationships respectively:

$$a_o\, V_{11} \cos\phi + V_{d1} \cos\psi/R_L' + g_{m2}E_2 = 0 \tag{14}$$

$$a_o\, V_{11} \sin\phi + V_{d1} \sin\psi/R_L' = 0 . \tag{15}$$

---

[1]The existence of a DC term arises from the fact that the two mixed voltages are of the same frequency. This is not the case with the conventional pentagrid converter, where the carrier frequency is much higher than that of the applied modulating signal.

Multiply Eq. (15) through by j and add the result to (14) in order to obtain a single complex equation in V_{11} and V_{d1}:

$$a_o V_{11}(\cos\phi + j\sin\phi) + (V_{d1}/R_L')(\cos\psi + j\sin\psi) + g_{m2}E_2 = 0$$

$$a_o V_{11}e^{j\phi} + (V_{d1}/R_L')e^{j\psi} + g_{m2}E_2 = 0$$

$$a_o \bar{V}_{11} + \bar{V}_{d1}/R_L' + g_{m2}E_2 = 0 \tag{16}$$

From Eq. (7) and (16) we can eliminate $\bar{V}_d$ to obtain $\bar{V}_{11}$ alone:

$$\bar{V}_{11} = \frac{-j\omega C_{gd}\bar{Z}_1 g_{m2}R_L' E_2}{1 + j\omega C_{gd}\bar{Z}_1(1 + a_o R_L')} \cdot \tag{17}$$

Now the dc component of drain voltage V_{do} is related to V_{11} through Eq. (12):

$$V_{do} = -(1/2)a_1 R_L' V_{11}\cos\phi = -(1/2)a_1 R_L' \, \mathrm{Re}\{\bar{V}_{11}\}$$

$$= -(1/2)a_1 R_L' \, \mathrm{Re}\left\{\frac{-j\omega C_{gd}\bar{Z}_1 g_{m2}R_L' E_2}{1 + j\omega C_{gd}\bar{Z}_1(1 + a_o R_L')}\right\}. \tag{18}$$

With the aid of Eqs. (1) and (4) we obtain the final expressions for the DC components of drain voltage V_{do} and drain current I_{do}.

$$V_{do} = -\frac{a_1 R_L' C_{gd} g_{m2} R_L' E_2}{2C}\left[\frac{(1 - \omega^2 P/\omega_o^2)Q^2}{1 + (1 - \omega^2 P/\omega_o^2)^2 \omega_o^2 Q^2/\omega^2}\right] \tag{19}$$

$$I_{do} = V_{do}/R_L$$

$$= -\frac{a_1 C_{gd} g_{m2} R_L E_2}{2C}\left(\frac{r_d}{r_d + R_L}\right)^2\left[\frac{(1 - \omega^2 P/\omega_o^2)Q^2}{1 + (1 - \omega^2 P/\omega_o^2)^2 \omega_o^2 Q^2/\omega^2}\right] \tag{20}$$

where $P \equiv 1 + (C_{gd}/C)(1 + a_o R_L')$. (21)

Because in practice the second term in Eq. (21) is small, the dimensionless quantity P is close to unity. Figure 4 shows a plot of the normalized load current $i = I_{do}/I_R$ versus ω/ω_o for several values of Q and for P = 1. The quantity I_R, having the dimension of current, consists of the factors preceeding the fraction in Eq. (20):

$$I_R = - \frac{a_1 C_{gd} g_{m2} R_L E_2}{2C} \left(\frac{r_d}{r_d + R_L} \right)^2 . \tag{22}$$

The converter is tuned to $\omega/\omega_o = 1$ in the absence of sound and operates in the region between the positive and negative peaks. The presence of sound causes variations in ω_o, which in turn lead to variations in I_{do} at the sound frequency. We note that the converter will respond to changes in static pressure (through changes in ω_o) and is therefore suitable for sonic boom measurements, where very low frequencies are encountered.

When the microphone is not excited the total DC component of the FET drain current I_{do}' acually consists of two parts:

$$I_{do}' = I_Q + I_{do}, \tag{23}$$

where I_Q is the quiescent current and I_{do} the "mixing" current given by Eq. (20).

B. Properties of the Converter

1. Dynamic range. Let us rewrite Eq. (20) in normalized form, using $y = \omega^2/\omega_o^2$:

$$i = I_{do}/I_R = \frac{(1 - yP)Q^2}{1 + (1 - yP)^2 Q^2/y} \tag{24}$$

The location of the positive and negative peaks of the transfer function are found upon setting

$$\frac{\partial i}{\partial y} = 0,$$

which yields

$$y_{max} = Q/(PQ + \sqrt{P}) \tag{25}$$

$$y_{min} = Q/(PQ - \sqrt{P}) . \tag{26}$$

Upon substituting (25) and (26) into (24) we obtain

$$i_{max} = \sqrt{P}Q^2/(2PQ + \sqrt{P})$$

$$i_{min} = -\sqrt{P}Q^2/(2PQ - \sqrt{P}) .$$

Because of the difference in sign in the denominator the magnitudes of the two peaks are not quite the same. Furthermore, since $P \simeq 1$, $Q >> 1$,

$$\begin{cases} i_{max} \\ \\ i_{min} \end{cases} = \pm Q/2\sqrt{P}$$

whence

$$\begin{cases} I_{do\ max} \\ \\ I_{do\ min} \end{cases} = \pm I_R Q/2\sqrt{P} .$$

The dynamic range will depend upon the difference between these two values:

$$\Delta I_{do} = I_{do\ max} - I_{do\ min} = I_R Q/\sqrt{P} .$$

Thus for wide dynamic range we want to make I_R and Q as large as possible.

2. Shift in resonant frequency and separation of the peaks. The system is at resonance when $i = 0$, and from Eq. (24) we find that this condition is fulfilled when

$$1 - yP = 0$$

or equivalently

$$\omega_1 = \omega_o\sqrt{y} = \omega_o/\sqrt{P} .$$

Because P is slightly greater than unity, the resonant angular frequency ω_1 of the converter is slightly less than that of the isolated tank circuit.

From Eqs. (25) and (26) we determine the separation of the peaks on the angular frequency axis to be

$$\Delta\omega = \omega_{min} - \omega_{max} = \omega_o Q\sqrt{P}/(P^2Q^2 - P)$$

$$\simeq \omega_o/Q \qquad (P \simeq 1,\ Q >> 1). \tag{27}$$

If the transfer function is determined experimentally, then Eq. (27) provides a ready means of determining the Q of the tank circuit.

3. Conversion gain. We define the conversion gain G as

$$G = \frac{dI_{do}}{dC_o} = I_R \frac{\partial i}{\partial y}\frac{dy}{dC_o}$$

$$= \frac{I_R}{C}\frac{[(1 - yP)^2Q^2 - y^2P]Q^2}{[y + (1 - yP)^2Q^2]^2}\ . \tag{28}$$

The latter expression for G is obtained with the aid of (24) and the definition of y. For small changes in y about the resonance point $y = 1/P$, we may approximate (28) as follows:

$$G = -I_R PQ^2/C.$$

Thus the gain depends strongly upon Q because of the quadratic relationship. For high gain both I_R and Q should be as large as possible.

C. Experimental verification of the Transfer Function

For the purpose of testing the validity of the theoretical expression (20) the condenser microphone was replaced by a variable capacitor, such that a substantial portion of the transfer function could be traversed. Several data points -- line current I_{Lo} (entering point A, Fig. 2) versus capacitance C_o -- were taken. In a separate experiment it had been determined that the line current varies nearly proportionally with the FET drain current I_{do}' over the whole range of interest, the gain being 2.60:

$$I_{do}' = I_{Lo}/2.60. \tag{29}$$

Futhermore, the frequency ratio ω/ω_o is related to the capacitance ratio C_o/C as follows:

$$\omega/\omega_o = \sqrt{C_o/C} \quad . \tag{30}$$

The static capacitance C was taken to be the average of the values of capacitance at maximum and minimum I_{Lo}.

The theoretical value of I_{do}' is obtained from Eqs. (20), (23), and (37):

$$I_{do}' = I_Q + I_R \frac{(1 - C_oP/C)Q^2}{1 + (1 - C_oP/C)^2CQ^2/C_o} \quad . \tag{31}$$

For each setting of the variable capacitor C_o the line current was found by measuring the voltage across a 274 Ω resistor with a Fluke Model 8300A Digital Voltmeter. Then the capacitor was removed from the converter and the capacitance measured on a ESI Model 250DE Impedance Bridge.

For the theoretical transfer function (30) Q was determined through Eq. (27), P set equal to unity, and I_Q and I_R found from the best fit to the experimental values by the method of least squares. The result for Converter 1, along with the experimental data points, is shown in Fig. 5. The values of Q, I_Q, and I_R, as obtained by the procedures just described, are given in the caption. The closeness of the fit between theory and experiment substantiates the validity of the circuit model and analysis, and indicates that we have an excellent understanding of the behavior of the converter.

The value Q = 15.6 listed in Fig. 5 is much lower than the value Q = 45 for the isolated inductor, as measured on a Boonton Q Meter. Likewise the Q of Converter 2 was determined to be 20.4 by Eq. (27), but the Q of its isolated inductor measured 150 on the Boonton Q Meter. The reason for these discrepancies remains unexplained.

D. Determination of the Conversion Transconductance

The parameters entering Eq. (20) can be obtained directly from the manufacturers' specification sheets or from the circuit conditions, with the exception of the conversion transconductance a_1. In order to compute this parameter we must have a plot of gate 1 transconductance g_{m1} versus gate 2 voltage v_2. This data for the Texas Instruments Type 3N202 is given in Fig. 6.

Let us expand g_{m1} in a Taylor series about the inflection point 0, about which we assume the function $g_{m1}(v_2)$ is antisymmetric:

$$g_{m1} = b_o + b_1(v_2 - V_o) + b_3(v_2 - V_o)^3 \tag{32}$$

$$\frac{\partial g_{m1}}{\partial v_2} = b_1 + 3b_3(v_2 - V_o)^2 .$$

Obviously b_o equals the value of g_{m1}, and b_1 the value of the slope $\frac{\partial g_{m1}}{\partial v_2}$, at the inflection point $v_2 = V_o$.

To find b_3 consider two arbitrary points (v_A, g_A) and (v_B, g_B):

$$g_A = b_o + b_1(v_A - V_o) + b_3(v_A - V_o)^3$$

$$g_B = b_o + b_1(v_B - V_o) + b_3(v_B - V_o)^3,$$

which yield

$$b_3 = \frac{g_A - g_B - b_1(v_A - v_B)}{[(v_A - V_o)^3 - (v_B - V_o)^3]} .$$

All the quantities in this expression are known.

If the FET is biased to operate about point C in Fig. 6., then

$$v_2 = V_c + E_2 \cos\omega t . \tag{33}$$

Upon substituting (33) into (32) we obtain

$$g_{m1} = b_o + b_1(V_c - V_o + E_2 \cos\omega t) + b_3(V_c - V_o + E_2 \cos\omega t)^3 . \tag{34}$$

We compare (34) to the Fourier series (9):

$$g_{m1} = a_o + a_1 \cos\omega t + a_2 \cos 2\omega t + \ldots$$

Equating the dc terms of these two series yields

$$a_o = b_o + b_1(V_C - V_o) + (3/2)b_3(V_C - V_o)E_2^2 + b_3(V_C - V_o)^3. \tag{35}$$

$$a_1 = \frac{\omega}{\pi}\int_0^{2\pi/\omega} g_{m1}(t)\cos\omega t\, dt$$

$$= b_1E_2 + 3b_3(V_C - V_o)^2E_2 + (3/4)b_3E_2^3 . \tag{36}$$

We can evaluate b_o, b_1, and b_3 with the aid of Fig. 6:

$$b_o = g_{m1}(V_o) = 5.1 \times 10^{-3} \text{ mho}$$

$$b_1 = \left.\frac{\partial g_{m1}}{\partial v_2}\right]_{V_o} = 5.1 \times 10^{-3} \text{ mho/volt}$$

$$b_3 = \frac{g_A - g_B - b_1(v_A - v_B)}{[(v_A - V_o)^3 - (v_B - V_o)^3]} = -0.6 \times 10^{-3} \text{ mho/V}^3.$$

If the amplitude of the carrier voltage $E_2 = 2$ V, then from Eq. (36) we obtain

$$a_1 = 3.0 \times 10^{-3} \text{ mho.}$$

With the values $a_1 = 3.0 \times 10^{-3}$ mho, $C_{gd} \simeq 2$ pf, $C = 19.6$ pf, $g_{m2} = 2 \times 10^{-3}$ mho, $r_d = 5 \times 10^4\ \Omega$, $E_2 = 2$ V, Eq. (22) yields $I_R = -0.27$ mA. This is in good agreement with the experimental value $I_R = -0.21$ mA (see Fig. 5); the difference is attributable to the uncertainty in the assumed value for C_{gd}, which is believed to consist primarily of lead capacitance.

IV. PROPERTIES AND SPECIFICATIONS

A. Converter Noise

The third octave noise spectrum from 25 Hz to 40 kHz and the linear (unweighted) noise spectrum in the band 22.4 Hz to 22.4 kHz were measured on each converter with the aid of a B&K Type 3347 Real-Time 1/3 Octave Analyzer. For all noise measurements the sensitivity switch of the zero drive amplifier was set to "10-100", the vernier to 1.0, and the gain switch to the desired range. The high-pass bypass (2Hz) and 20 kHz low-pass filters were plugged into the amplifier. The measurements proceeded as follows:

Step 1. A B&K Type 4133 1/2" condenser microphone was screwed onto the converter, and the output of the zero drive amplifier was connected to the 1/3 octave analyzer.

a. The converter was inserted into a Whittaker Model PC-125 Acoustic Calibrator, on which the sound pressure level was adjusted to 100 dB at 1 kHz.

b. The converter was tuned to produce maximum signal on the 1/3 octave analyzer.

c. By means of the "Digital Reference Adjust" and "Gain Control" switches the reading on the 1/3 octave analyzer was set to 100 dB.

d. The acoustic calibrator was turned off and a 33 Ω resistor inserted between the converter and the zero drive amplifier. The quiescent line current of the converter was determined by means of a voltage measurement across the 33 Ω resistor with a Hewlett-Packard Type 3480B Digital Voltmeter.

Thus the system was calibrated to measure electrical signals from the converter in terms of equivalent absolute sound pressure levels (re 2×10^{-5}

newton/m^2).

Step 2. The condensor microphone was replaced by a dummy microphone, a fixed capacitor inside a B&K Type JJ2614 Adapter (capacitance = 23 pf), in order to eliminate signals generated by ambient sound and vibration.

a. The converter was retuned to establish the same quiescent line current as in Step 1d. This step is necessary because deviations from the optimal operating point produce excess noise in the converter (see below).

b. The 33 Ω resistor was removed and the converter noise level recorded on each of the 1/3 octave bands as well as on the linear 22.4 Hz to 22.4 kHz band.

The noise spectrum of Converters 1 and 2, with the zero drive amplifier on the 100 range, are shown in Figs. 7 and 8 respectively. The noise levels are fairly uniform across the entire spectrum, including those in the bands containing 60 Hz and harmonics thereof. The noise level in the linear band 22.4 Hz to 22.4 kHz (henceforth designated as the "wideband" noise) is shown in the column marked "Lin." The wideband noise levels for various amplifier range settings are shown in Table I. As can be seen, the 100 range setting does not provide the lowest system noise, but it is the lowest setting that will accommodate the full dynamic range of the converter.

Fig. 9 shows the noise spectrum with a 1000' cable -- Belden 8761-1000 22 AWG stranded twisted pair, beldfoil shielded (shield floating) -- between Converter 2 and the zero drive amplifier. The cable actually brings about a decrease in the wideband noise, the greater improvement lying in the lower frequency bands. We conclude, then, that a long cable will not be detrimental to the system, even at low sound pressure levels.

The contribution of the N400 Amplifier itself to the overall noise is difficult to assess. Fig. 10 shows the noise spectrum of the N400 amplifier

with the input open. Usually such measurements are made with the input shorted, but the 22V at the input terminals prevented this; nevertheless the noise remained unaffected by the presence of resistors or capacitors across the input. The wideband noise of the amplifier lies about 3 dB below that of the overall system and is thus not a major contributor, except perhaps in the higher frequency bands.

Finally, the dependence of the wideband noise upon the quiescent line current is brought out in Fig. 11. The noise rises sharply as the quiescent current deviates from its optimum value, and this is an important reason for compensating the converter against changes in line current with temperature.

b. Distortion and Linearity

The percent distortion d of a signal containing harmonic amplitudes A_1, A_2, A_3, ... is defined as follows:

$$d = \frac{(|A_2|^2 + |A_3|^2 + |A_4|^2 + \ldots)^{1/2}}{(|A_1|^2 + |A_2|^2 + |A_3|^2 + \ldots)^{1/2}} \times 100$$

$$\simeq \frac{(|A_2|^2 + |A_3|^2 + |A_4|^2 + \ldots)^{1/2}}{A_1} \times 100$$

$$\text{if } A_1 \gg A_2, A_3, \ldots \qquad (37)$$

The distortion measurements were made on a Hewlett-Packard Model 334A Distortion Analyzer. With this instrument we first measure the rms value of the total signal [denominator of Eq. (37)] and normalize the meter reading to unity. Then we filter out the fundamental component, measure the rms value of the remainder and read the meter directly in percent distortion. The Model PC-125 Acoustic Calibrator was used to provide the signals at 1000 Hz to the microphone. The distortion of Converters 1 and 2 with the N400 on the 100 range versus sound pressure level are shown in Fig. 12.

The 4% distortion level occurs at approximately 143 dB for Converter 1 and approximately 132 dB for Converter 2.

The rms output voltage was measured at each SPL. The plots of Fig. 13 illustrate the excellent linearity of both converters. Note that the conversion gain of Converter 1 is 10.5 dB below that of Converter 2, owing to the lower Q of its tank circuit.

C. Dynamic Range

In accordance with the specifications of manufacturers of acoustical instrumentation the dynamic range is defined to extend from 5 dB above the noise floor to the 4% distortion level. With the zero drive amplifier on the 100 range, the dynamic range of both converters spans 72 dB (see Table II).

D. Frequency Response

A University Sound Model ID-40A Heavy Duty Driver, activated by a variable frequency oscillator and power amplifier, was employed for the purpose of measuring the frequency dependence of the conversion gain. A coupler with an O-ring seal was constructed to seat the Type 4133 1/2" condenser microphone. At each measured frequency the microphone cartridge was screwed onto a B&K Type UA0039 Extension Connector, and the SPL was measured on a Type 2203 Precision Sound Level Meter. The driver output was adjusted to a prescribed SPL. After the microphone cartridge was then screwed onto the converter and reinserted into the coupler, the output voltage of the converter-N400 system was measured. The frequency response at SPL's of 110 dB and 136 dB is shown in Fig. 14. In both cases the upper cutoff frequency (-3dB point) lies at 28 kHz. The system response

remains flat down to at least 20 Hz, the lowest frequency at which the driver could be activated.

E. Temperature Stability

A series of tests were undertaken to determine the sensitivity of several converter properties to changes in ambient temperature. The converter under test was placed in an environmental chamber, in which the temperature could either be raised or lowered[2]. The temperature was measured with an iron-constantin thermocouple, the junction taped to the converter housing, and the leads connected to a Thermoelectric "Minimite" pyrometer indicator. The microphone cartridge was inserted into a B&K Type 4220 Pistonphone, which generates a 124 dB SPL at 250 Hz. The pistonphone was driven by an external power supply (HP Model 6299A) to prevent possible damage to the batteries over the range of temperatures covered (40-130°F). At each temperature were measured the converter line current, conversion gain, distortion (Converter 2 only), and noise spectrum.

The converter line current was obtained by measurement of the voltage across a 33 Ω resistor with a HP Model 3480B Digital Voltmeter. Figure 15 shows how the line current of both converters drifts with temperature. With this drift is associated a deterioration in the conversion gain and increase in distortion. If at a given temperature the converter is retuned to adjust the line current to its room temperature value, then the gain and distortion return to their room temperature values.

After measurement of the line current the 33 Ω resistor was removed and the pistonphone turned on. It is assumed that the pistonphone main-

---

[2]This chamber was made available through the courtesy of the Strain Gage Measurements Section, Langley Research Center.

tained a 124 dB SPL over the entire temperature range, because the two major contributions to changes in SPL -- thermal expansion and changes in the ratio of specific heats at constant pressure and constant volume -- are negligibly small (<0.1 dB). The temperature variation of the output voltage of the zero drive amplifier, measured in dB on the B&K Type 3347 1/3 Octave Analyzer, for a 124 dB SPL at the microphone is shown in Fig. 16. The distortion of Converter 2 was measured at several temperatures on the HP Model 334A Distortion Analyzer; these data are shown in Fig. 17.

The noise spectra of the converters were measured at several temperatures. The temperature controller and fan were shut off briefly for the noise spectrum to be recorded in the storage made of the 1/3 octave analyzer. Because it was impractical to replace the microphone with a dummy while the converter was in the chamber, the converter noise was markedly influenced by ambient sound and vibration. In fact, the wideband linear noise levels lay almost 15 dB above those described in Section A, but no significant dependence upon temperature was noted.

Thus it appears that the room temperature specifications are maintained only within a rather narrow range of temperatures, unless the converter is retuned. However, it must be borne in mind that these tests were undertaken with no temperature compensation built into the converter. A suggestion for such compensation is described in Part VI.

F. Miscellaneous

The following additional specifications are of interest.

1. Power drawn by converter from N400: 350 mW.
2. Unsuppressed carrier (9.008 MHz) at N400 output: <1mV on 100 range.

3. Voltage regulation:

   a) Converter is insensitive to line voltage between 19-28 V.

   b) N400 maintains 22 V. for line currents up to 25 mA.

Further specifications are listed in Table II.

V. COMPARISON WITH PRESENT SYSTEMS

The systems presently employed in the field by the Acoustical Vibrational Instrumentation Section are the General Radio 1" and General Radio 1/2" systems for aircraft noise, and the Photocon "Dynagage" system for sonic boom. These systems consist of the following components:

1. General Radio 1" System: P7 ceramic microphone, 1560-P40 preamplifier, 1551-CS3 sound level meter (modified).
2. General Radio 1/2" System: B&K Type 4134 1/2" condenser microphone, 1560-P42 preamplifier, 1551-CS3 sound level meter (modified).
3. Photocon System: Photocon 1" condenser microphone, Dynagage Model DG-6060, PS605 power supply.

Several specifications of these systems, as determined by our own measurements in the laboratory, and general features are listed in Table II.

The noise spectra were obtained in a manner similar to that described in IV A. First each system was fitted with its respective microphone, and its output voltage was calibrated in absolute dB with the aid of the PC-125 Acoustic Calibrator and the Type 3347 1/3 Octave Analyzer. Then the microphones were replaced by the dummy microphones listed below and the noise spectra measured on the 1/3 octave analyzer:

GR 1" System: 143 pf fixed capacitor,

GR 1/2" System: 23 pf fixed capacitor,

Photocon System: Photocon CT-4 variable capacitor.

The 200 V polarization voltage was turned on and the preamplifier gain was set on "X1" for the measurements of the GR systems. For the Photocon system the Dynagage was tuned to "55" for the calibration and retuned to this

figure with the CT-4. The noise spectra for the three systems, with the GR sound level meter set to 100 dB and the Dynagage set to 0 dB attenuation, are presented in Figs. 18, 19, and 20 respectively. The wideband noise for other settings is given in Table III. The GR systems were not tested on ranges below 70 dB.

The great forte of the GR systems lies in their remarkably low base noise floor (43 dB on the 70 dB range). For aircraft noise measurements, on the other hand, these systems suffer a severe disadvantage in their limited dynamic range. For example, we conclude from the data in Table III that the GR sound level meter on the 70 dB range would permit noise measurements in the restricted range 48-80 dB (5 dB above the noise floor to 10 dB above the SL meter setting). Take the case where the anticipated sound level of aircraft noise would reach, say, 120 dB. Accordingly we would set the sound level meter to 110 dB, where the noise floor fixes the lower end of the dynamic range at 74 dB, as opposed to the desired 60 dB. Furthermore, technicians in the field report unpredictable, spurious bursts of noise originating in the 1560-P42 preamplifier (but not in the 1560-P40); it is for this reason that the GR 1/2" system has been abandoned for this application [4]. The presence of the 200 V polarization voltage on the diaphram of the 1/2" condenser microphone, in addition, makes the system sensitive to ambient humidity, especially if condensation takes place.

The GR 1" system, on the other hand, is restricted in response to higher frequencies owing to the peculiar characteristic of ceramic microphones. With increasing frequency, the microphone response takes a dip and rises to a peak before finally reaching its high frequency cutoff. According to General Radio specifications, the difference between dip and peak levels may amount to as much as ±5 dB in the vicinity of 10 kHz [5]. The usefulness

of the microphone in this frequency region depends upon ones ability to calibrate the microphone response vs. frequency accurately and upon the desired accuracy of the measurement.

The Photon system displays excellent linearity and dynamic range. Most of its problems originate in the fact that the carrier travels the full length of the cable between the Dynagage and the microphone. First the system is highly sensitive to cable length and to the insulating material between conductors; as a result an impedance-matching network is required at the cable terminals. Secondly, cross-modulation, in the form of beats between adjacent units having slightly different carrier frequencies, is sometimes excessive. This system, like the proposed converter-zero drive system, responds to a static pressure change and is useful at the very low frequencies required for sonic boom measurements; nevertheless, the fact that it is designed exclusively for 1" condenser microphones limits its high frequency response to 10 kHz.

These three systems, together with the Converter 2-N400 System, were tested in the field on August 2, 1972, in order to determine the effects of long extended cables. The site selected was along Wythe Creek Road, just outside NASA-Langley Research Center. The cables, 1000' in length, lay straight beneath and parallel to several electric power lines. An attempt was made to answer the following three questions:

1. Are the systems susceptible to radio frequency pick-up, if a transmitter is operating in the vicinity of the cables? The source of the RF transmission in the test was a 15 watt range radio transmitting at 49.830 MHz.

2. What is the magnitude of the cross-modulation of the Photocon system and how does it compare to that of the converter-N400 system?

3. What is the magnitude of the pick-up from the overhead power lines (60 Hz and harmonics)?

A sufficient number of tests were performed to answer only the third question. After calibration with a HP Model 15117A Sound Level Calibrator, dummy microphones were inserted and, the noise spectra of the GR 1/2" system and the Converter 2-N400 system were measured. These spectra, shown in Figs. 21a and 21b, reveal extraordinarily large voltages in the 62, 160, and 200 Hz 1/3 octave bands, corresponding to the fundamental power line frequency and third harmonic. The pick-up on the Converter 2-N400 system is attributable to the fact that the shield of the 1000' cable was left floating, as necessitated by the grounding difficulty described earlier.

VI. SUGGESTIONS FOR ADDITIONAL FEATURES AND IMPROVEMENT

A. Converter

The following additional features may be readily incorporated in the converter for improvement of specifications or for operator convenience.

1. A third conductor may be added to the cable as a service wire, either for calibration or retuning if the microphone is situated at a remote location.

2. A converter constructed like Converter 2, having the tank circuit built into the UA0300 Input Adapter, can easily accommodate other than 1/2" microphones. The UA0300 would simply be replaced by a UA0035 for the 1/4" microphone, by a UA0036 for the 1/8" microphone, and by DB0375 for the 1" microphone. Each adapter, of course, must contain the appropriate coil for tuning the tank circuit to the carrier frequency.

3. The cause of the drift of drain current with temperatures has not yet been investigated; the drift may arise from either changes in the inductance L with temperature or from shifts in the operating point of the FET. A circuit for compensating against the latter is shown in Fig. 22. The resistors R_A and R_B impose a small positive bias voltage on gate 1 of the FET; capacitor C_A isolates the tank circuit from the bias network and is large enough to have negligible effect upon the tuning. With increasing temperature the common source characteristics of the n-channel MOSFET rise; this can be countered by lowering the positive bias voltage on gate 1, as may be realized by making R_B a thermistor or reverse-biased diode.

4. The addition of attenuation at the input can shift the dynamic range of the converters to higher SPL's. The first attempt consisted of an

added parallel 10 kΩ resistor to reduce the Q of the tank circuit; this however, resulted in excessive distortion, even at SPL's as low as 100 DB (3.8% distortion). The scheme of Fig. 23, where two capacitors C_1 and C_2 are added to the tank circuit, may prove satisfactory. If C_T is the combined capacitance of C_1, C_2, and the microphone C, and F the desired attenuation factor, then C_1 and C_2 are chosen to fulfill the following conditions:

$$C_T = C$$

$$\frac{\delta C_T}{C_T} = \frac{1}{F}\frac{\delta C}{C}.$$

An elementary analysis reveals that these are fulfilled by the following choice of C_1 and C_2:

$$C_1 = (\sqrt{F} - 1)C$$

$$C_2 = \frac{\sqrt{F}}{\sqrt{F} - 1} C.$$

For example, an attenuation of 20 dB (F =10) will require C_1 = 2.16C and C_2 = 1.46C. A switch built into the converter to switch the two additional capacitors in and out of the tank circuit would make possible the following set of dynamic ranges:

	Switch out	Switch in
Converter 1	71 - 143 dB	91 - 163 dB
Converter 2	60 - 132	80 - 152

B. Zero Drive Amplifier

The following changes are desirable in the N400 zero drive amplifier.

1. The recovery time from saturation must be reduced from 5 seconds (per present specification) to several milliseconds. For both aircraft noise and sonic boom measurements the system must be operational at the time

of flyover; a delay of several seconds in amplifier recovery may result in the omission of essential data.

2. The low frequency response of the amplifier, containing the high-pass bypass filter, should be lowered from the present 2 Hz to at least 0.02 Hz for sonic boom measurements.

3. The voltage at the inner input conductor should be positive with respect to signal ground in order to eliminate the problem of properly grounding the converters.

4. A 2 dB stepping switch would be preferred over the present vernier control for amplifier attenuation. This feature is already built into the Model N460 Hydrophone Amplifier with 1 dB steps.

VII. CONCLUSIONS

Laboratory tests and preliminary field tests have demonstrated the capability of the converter-zero drive system, developed under this research grant, to meet the stringent NASA requirements in aircraft noise and sonic boom instrumentation. Let us reconsider the specifications listed at the beginning of this report:

a) Frequency response. The frequency response of the converter itself, dc-28 kHz, meets specifications; the 2 Hz low frequency cutoff is a limitation of the zero drive amplifier.

b) Dynamic range. The 72 dB dynamic range of the system slightly exceeds the specified 70 dB. A range switching network has been proposed to fulfill the requirements for both aircraft noise and sonic boom with the same unit.

c) Insensitivity to cable length and type. A change in cable length from about 2' to 1000' produced no marked change in converter performance, except for a slight decrease in noise.

d) Insensitivity to ambient temperature and humidity. The converter, without any built-in temperature compensation, exhibits a deterioration in performance with changes in ambient temperature. This remains as an object for further investigation. The converter should prove less sensitive to ambient humidity than the preamplifiers requiring a polarization voltage.

A theoretical analysis of the converter circuit shows excellent agreement with experimental results. A major discrepancy, however, lies in the values of Q obtained from the transfer function and from an independent measurement on a Q meter. A summary of the theoretical analysis and

experimental results will be submitted for publication in the IEEE Transactions on Instrumentation and Measurement.

Additional advantages of the converter include those inherent in solid state construction: ruggedness, endurance, small size, light weight, and low power requirements. Furthermore, removal of the carrier at the microphone eliminates cross-talk and problems associated with proper termination of a long cable. Finally the converter-N400 system provides a single system for measuring both aircraft noise and sonic boom; only a minimum of adjustment will be necessary, such as changing microphone cartridges and changing input attenuation, in switching from one type of measurement to the other.

Further developmental work will be required in improving the low frequency response and reversing the polarity of the zero drive amplifier, in providing temperature compensation for the converter, and in constructing adapters for microphones of different sizes.

Several of the laboratory tests will comprise the substance of the master's thesis of the graduate research assistant assigned to the project. A Disclosure of Invention (NASA Form 235), describing the converter, will be submitted to the Office of Patent Counsel, Langley Research Center.

REFERENCES

[1] W. Alexander, Electronic Engineering, Vol. 23, p. 479, 1951.

[2] J. E. Judd and E. P. Moran, "A New Differential Zero Drive System for Direct Wideband Audio Data Transmission Over Standard Telephone Lines," Reprint M68-1, MB Electronics, New Haven, Conn.

[3] F. E. Terman, Electronic and Radio Engineering. New York: McGraw-Hill, 1955, p. 479.

[4] Private communication.

[5] General Radio Catalog V, February 1970, p. 25.

Table I. Noise of Converter-N400 System vs. Amplifier Range Setting

Bandwidth: 22.4 Hz-22.4 kHz

Weighting: linear

N400 Range	Converter 1 Noise	Converter 2 Noise
10	63.4 dB	53.0 dB
30	63.2	52.2
100	65.6	54.6
300	71.0	60.0

Table II. Specifications of Systems Used in Measurement of Aircraft Noise and Sonic Boom.

Specification \ System		Converter 1-N400	Converter 2-N400	General Radio 1"	General Radio 1/2"	Photocon
Microphone		1/2" [1]	1/2" [1]	1"	1/2"	1"
Cable		2 conductor shielded	2 conductor shielded	2 conductor shielded	2 conductor shielded	1 conductor shielded
Termination network		None	None	Booster Amplifier	Booster Amplifier	Impedance matching network
Carrier frequency		9 MHz	9 MHz	None	None	700 kHz
Polarization voltage		None	None	200 V	200 V	None
Unsuppressed carrier		1mV P-P	1mV P-P	None	None	1-5 mV P-P
Frequency response		2 Hz-28 kHz [2]	2 Hz-28 kHz [2]	20 Hz-10 kHz	20 Hz-20 kHz	dc-10 kHz
Noise floor, best range [3]		63.2 dB	52.2 dB	43.0 dB	43.0 dB	50.4 dB
System set on range to measure 130 dB SPL	Noise floor [4]	65.6 dB	54.6 dB	77.8 dB	77.6 dB	54.8 dB
	SPL @ 4% distortion	143. dB	132 dB	130 dB [5]	130 dB [5]	137 dB
	Dynamic range [6]	72 dB (71-143)	72 dB (60-132)	47 dB (83-130)	47 dB (83-130	77 dB (60-137)
	RMS output voltage @ 124 dB SPL	0.85 V	2.7 V	0.53 V	0.51 V	1.1 V

Notes: All footnotes on following page.

FOOTNOTES TO TABLE II.

1) Tank circuit can be changed to accommodate other sizes.

2) Lower frequency cutoff is limited by the N400 amplifier. The converters themselves will respond to static pressure change.

3) Noise measurements are unweighted (linear), 22.4 Hz-22.4 kHz. Best ranges are as follows:

   Converters 1 and 2: N400 on 30 range.

   General Radio: sound level meter on 70 dB setting.

   Photocon: Dynagage attenuation = 0 dB.

4) Ranges for measuring 130 dB SPL are the following:

   Converters 1 and 2: N400 on 100 range.

   General Radio: sound level meter on 120 dB setting.

   Photocon: Dynagage attenuation = 6 dB.

5) General Radio systems are limited by maximum meter reading, rather than by distortion.

6) 5 dB above noise floor to 4% distortion level.

Table III. Noise of Present Systems vs. Range Setting

Bandwidth: 22.4 Hz-22.4 kHz

Weighting: linear

A. General Radio

SL Meter Range	GR 1" System Noise	GR 1/2" System Noise
70		43.0 dB
80		44.8
90		49.8
100	58.2 dB	57.6
110	69.0	68.8
120	77.8	77.6
130	87.6	88.6
140	96.4	97.2

B. Photocon

Dynagage Attenuation	Photocon System Noise
0 dB	50.4 dB
6	54.8

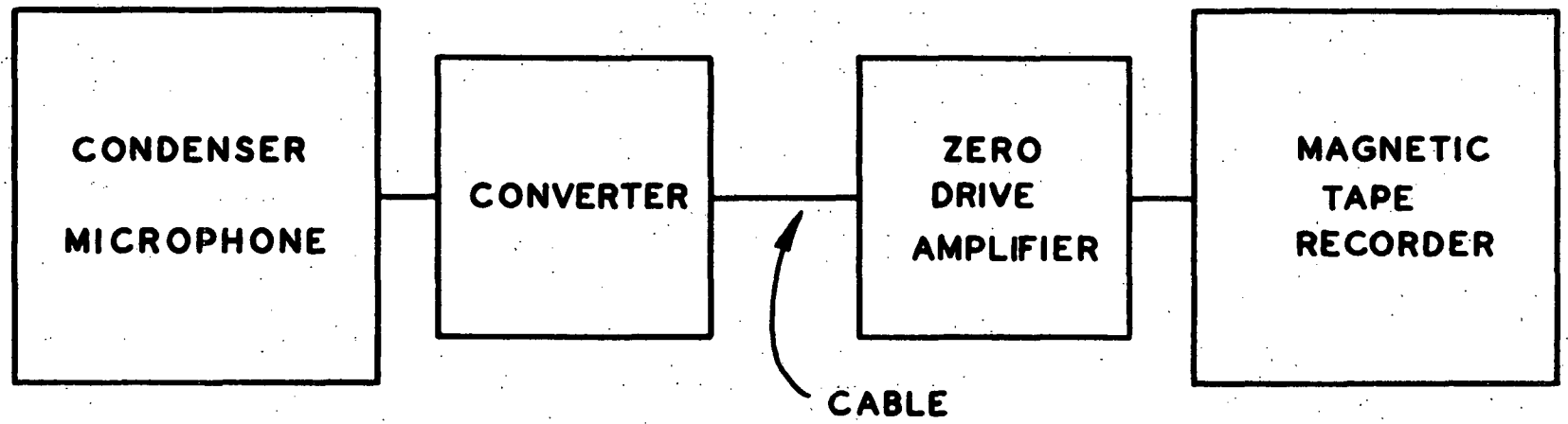

Fig. 1. Block diagram of the proposed system for measuring aircraft noise and sonic boom.

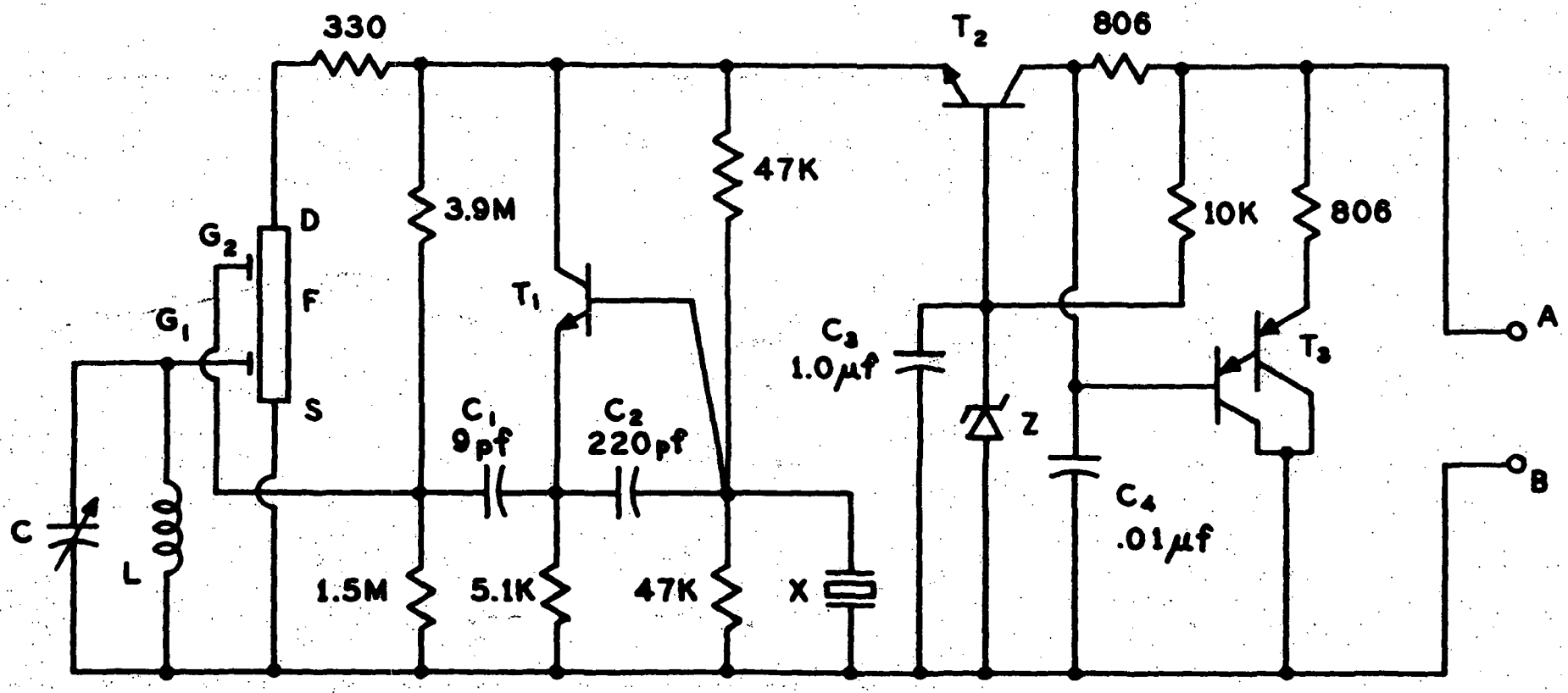

NOTES: 1. ALL RESISTORS 1/4 WATT

2. TERMINALS A-B CONNECTED TO INPUT MB ELECTRONICS N400 ZERO-DRIVE AMPLIFIER

Fig. 2. Circuit diagram of the solid state converter. Legend: L 14-18μH variable inductor (Converter 1), 12μH fixed inductor (Converter 2); C condenser microphone (cartridge capacitance = 18.6pf; add 0.8-8pf variable capacitance for Converter 2); F 3N202 dual-gate MOSFET; T_1 2N3711 transistor; T_2 2N930 transistor; T_3 S9120 Darlington transistor; Z 1N759A zener diode; X Reeves-Hoffman RHA5A quartz crystal (9.008 MHz).

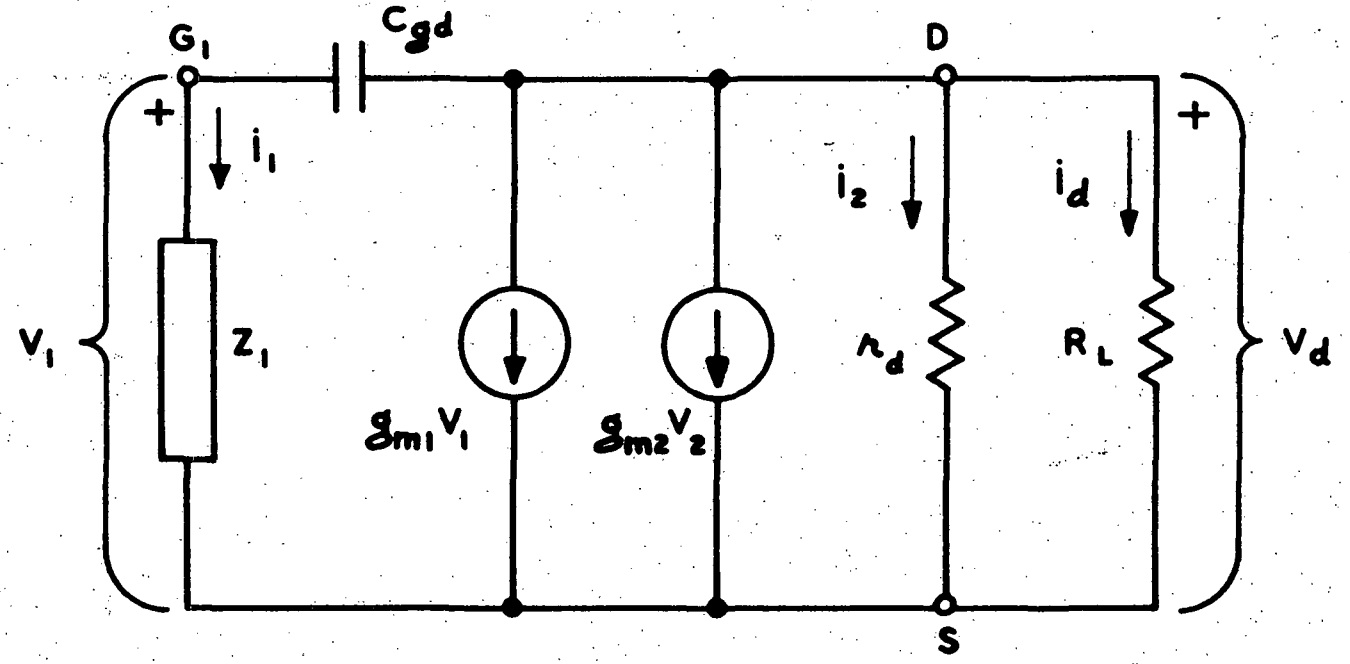

Fig. 3. Circuit model of dual-gate field-effect transistor with terminal connections.

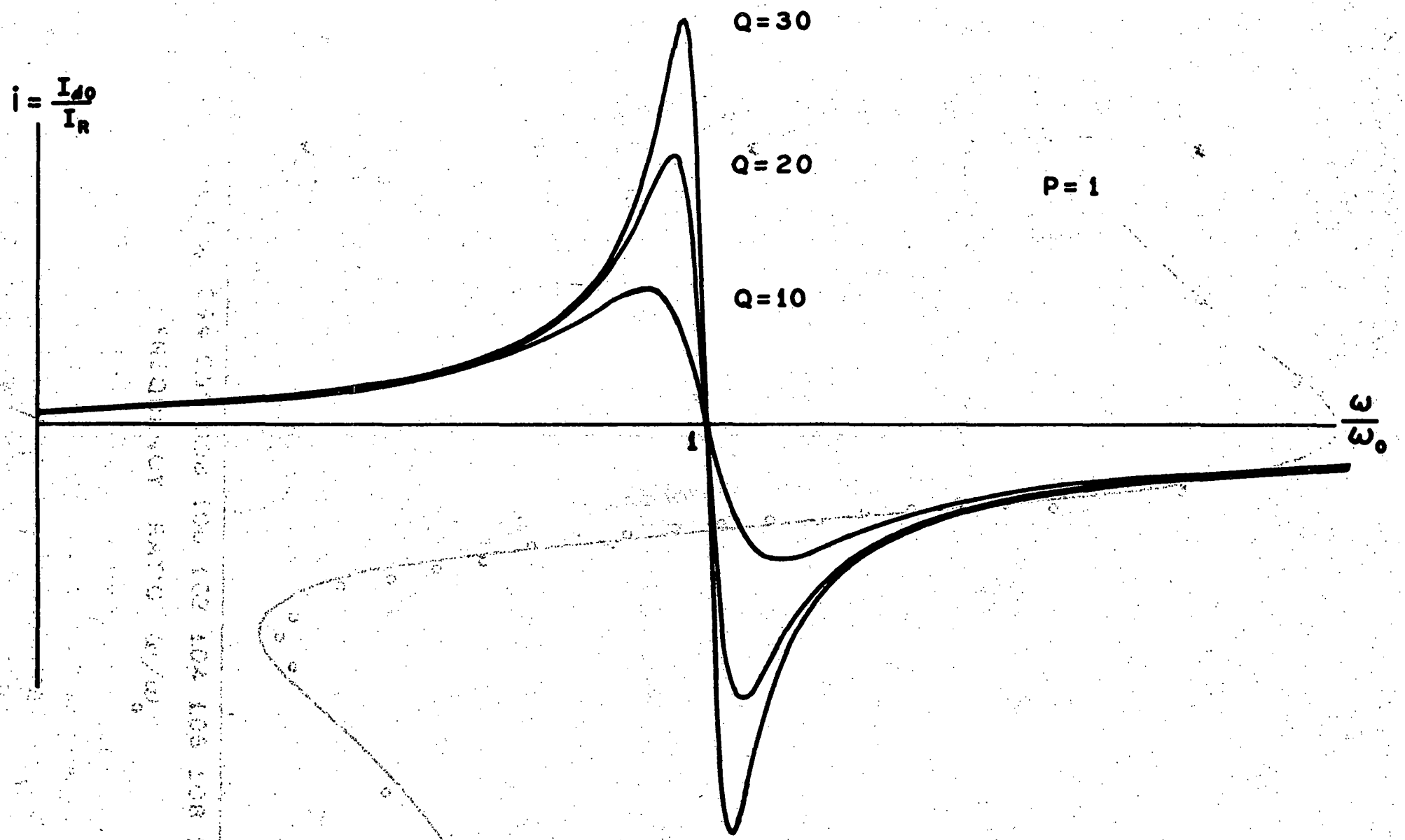

Fig. 4. Transfer function of converter for P = 1 and three different values of Q.

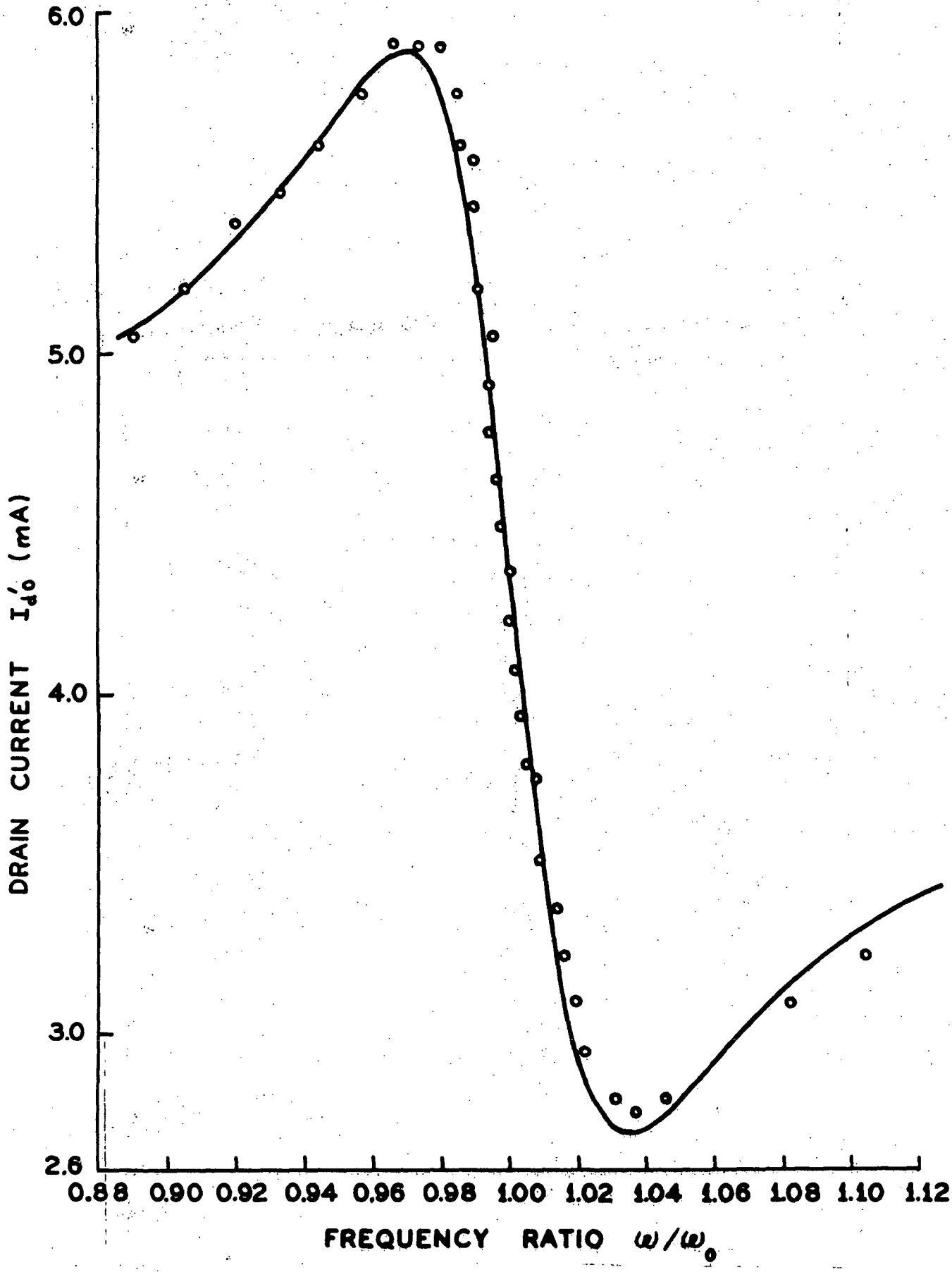

Fig. 5. Comparison of theoretical transfer function (solid curve) with experimental values (circles) for Converter 1; P was taken equal to unity, and the values Q = 15.6, I_Q = 4.353 mA, and I_R = -0.2050 mA were determined by best fit.

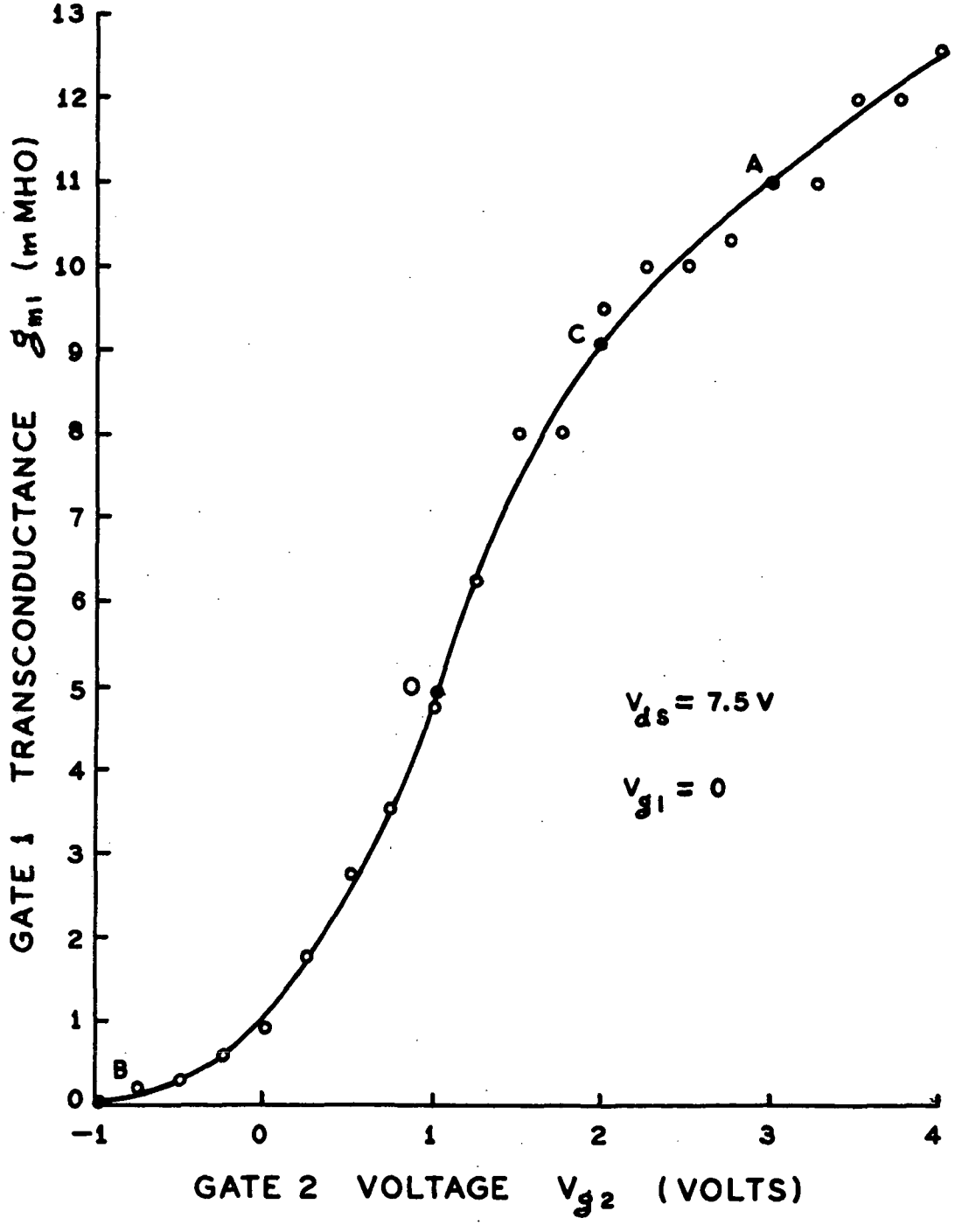

Fig. 6. Gate 1 transconductance versus gate 2 voltage for the 3N202 MOSFET.

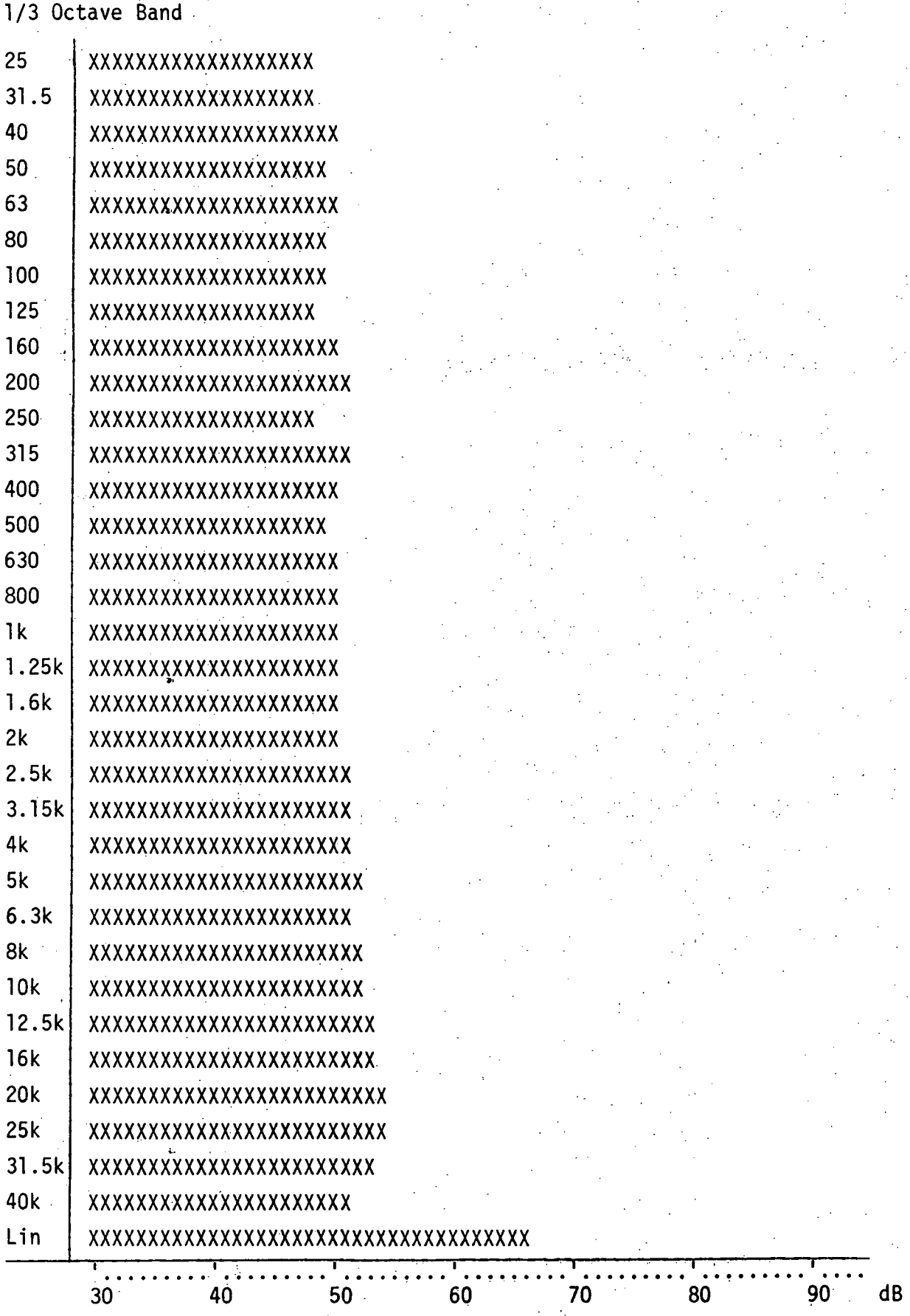

Fig. 7. Noise spectrum of Converter 1 with N400 on 100 range.

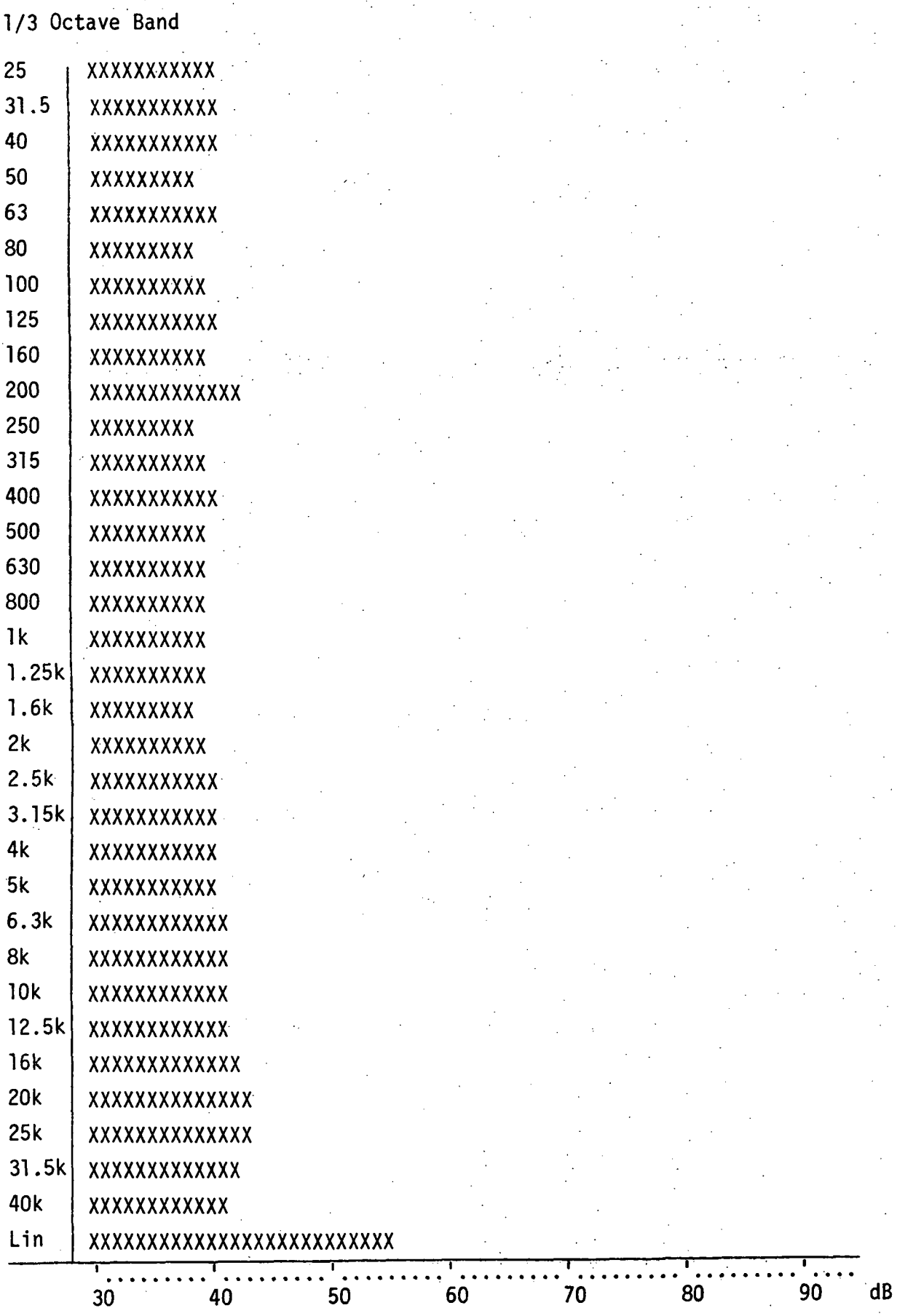

Fig. 8. Noise spectrum of Converter 2 with N400 on 100 range.

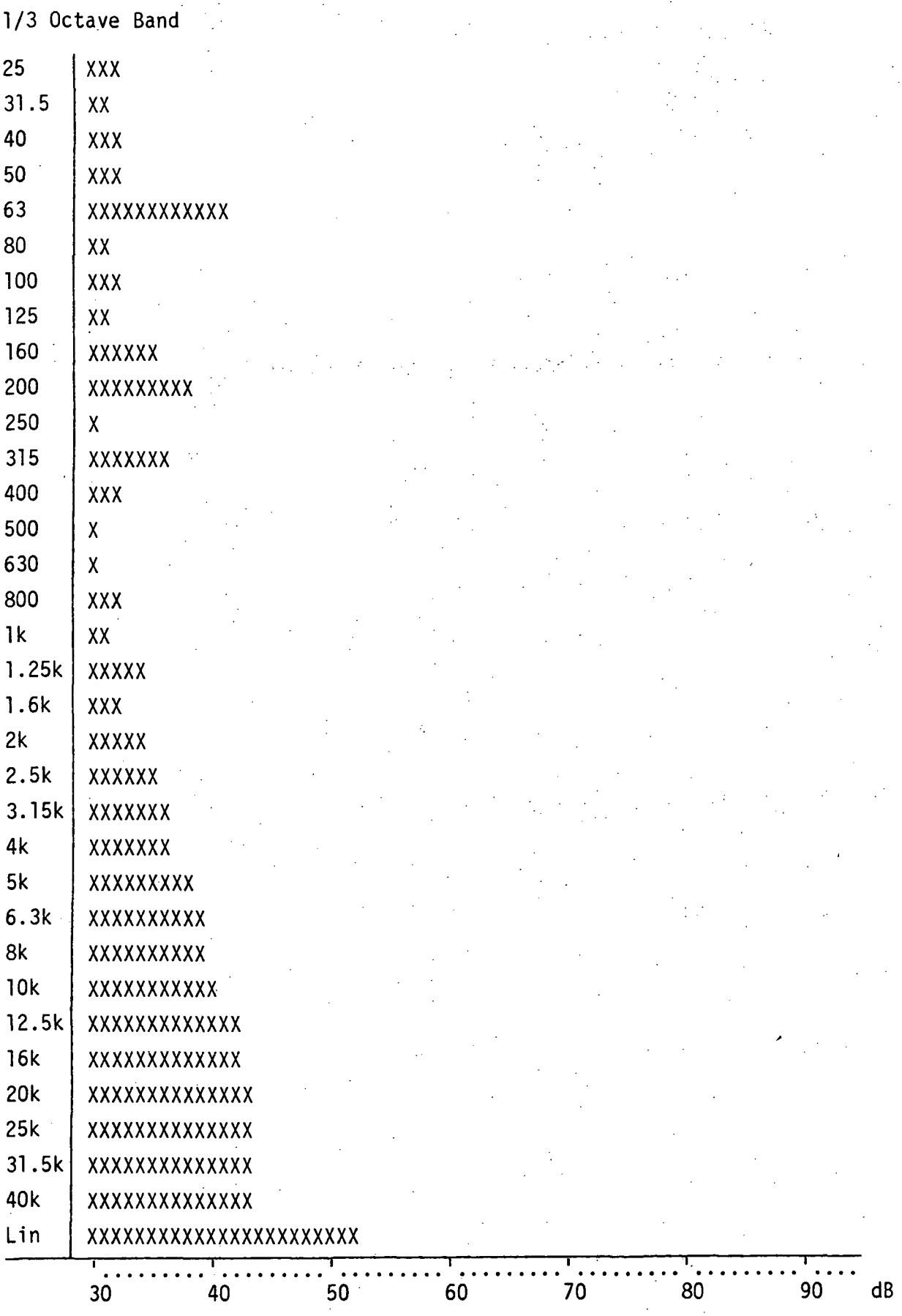

Fig. 9. Noise spectrum of Converter 2 over 1000' cable (N400 on 100 range).

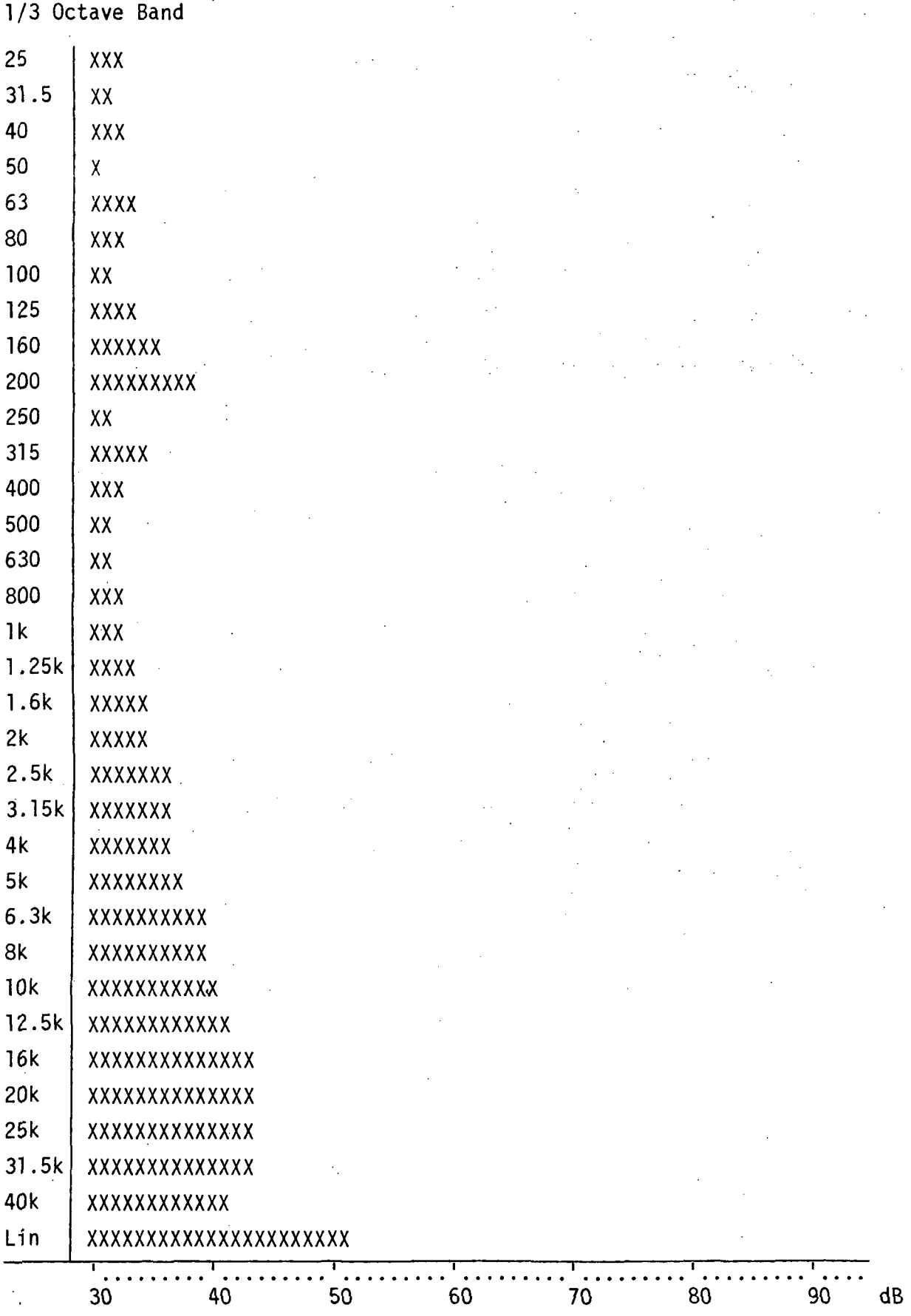

Fig. 10. Noise spectrum of N400 zero drive amplifier with input open (on 100 range).

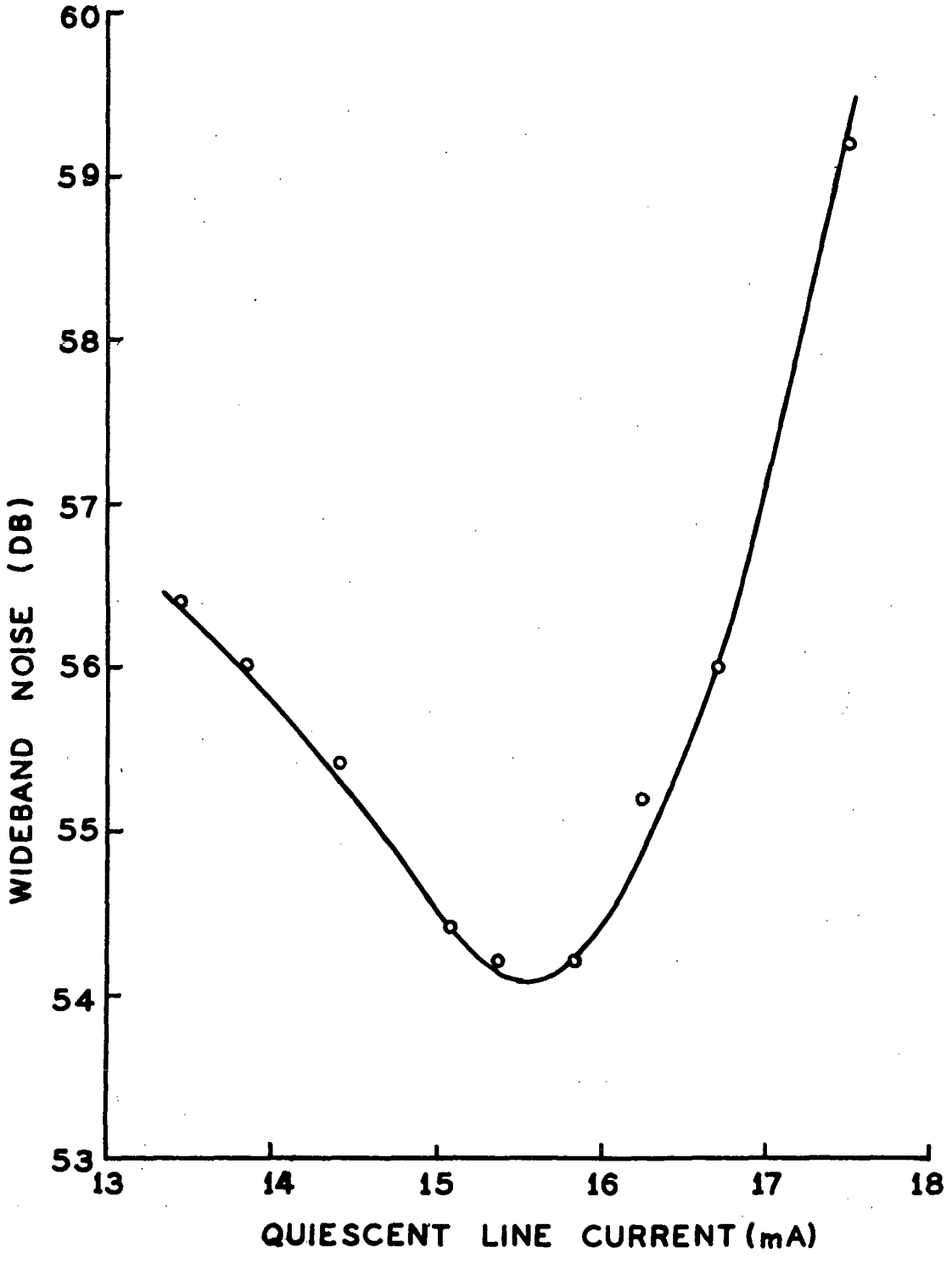

Fig. 11. Wideband noise (linear 22.4 Hz - 22.4 kHz) of Converter 2 versus quiescent line current (N400 on 100 range).

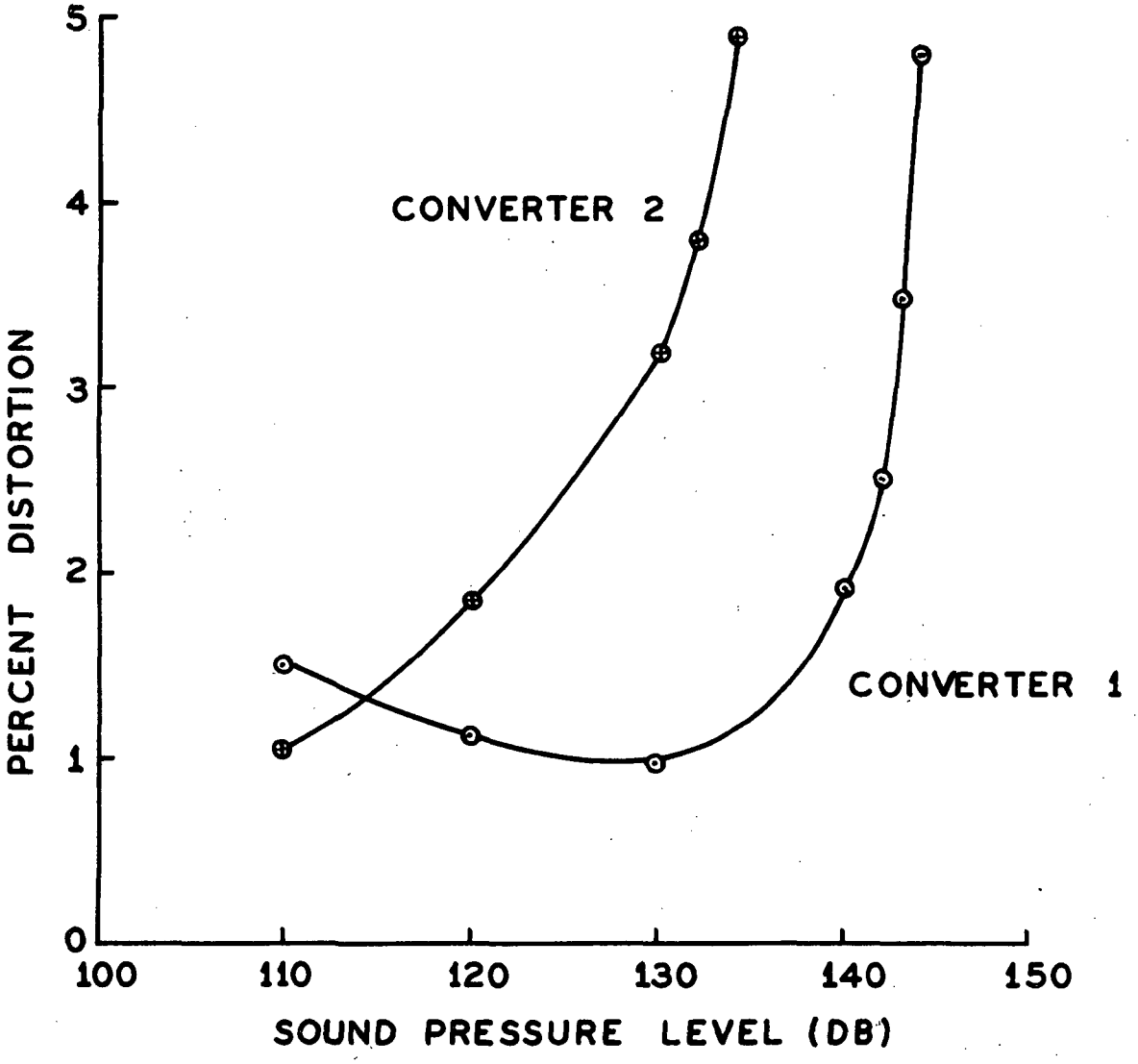

Fig. 12. Distortion of converter output versus sound pressure level (N400 on 100 range). The quiescent line currents are 14.1 mA for Converter 1 and 14.9 mA for Converter 2.

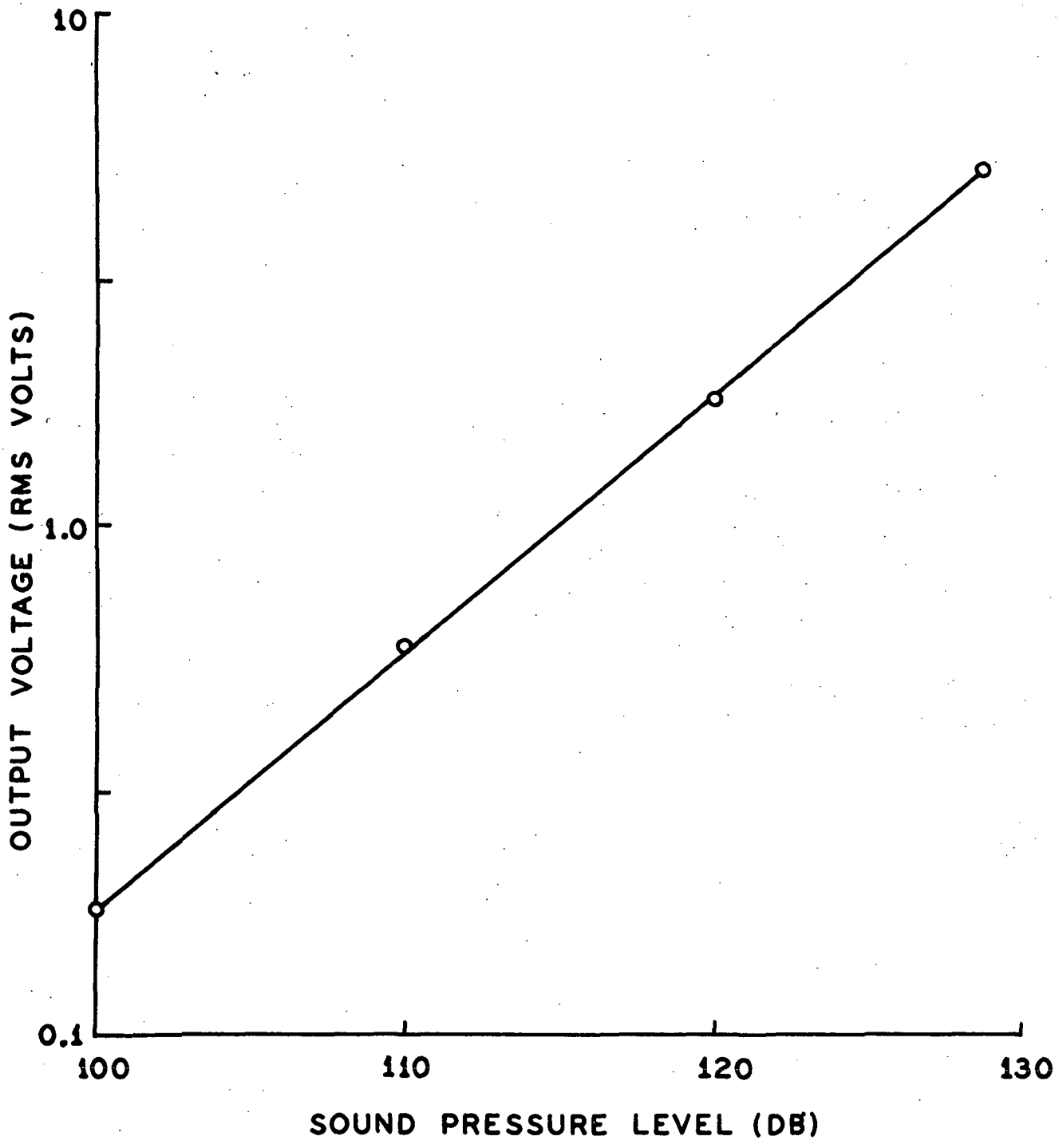

Fig. 13. Output voltage of Converter 2 - N400 System versus sound pressure level (N400 on 100 range).

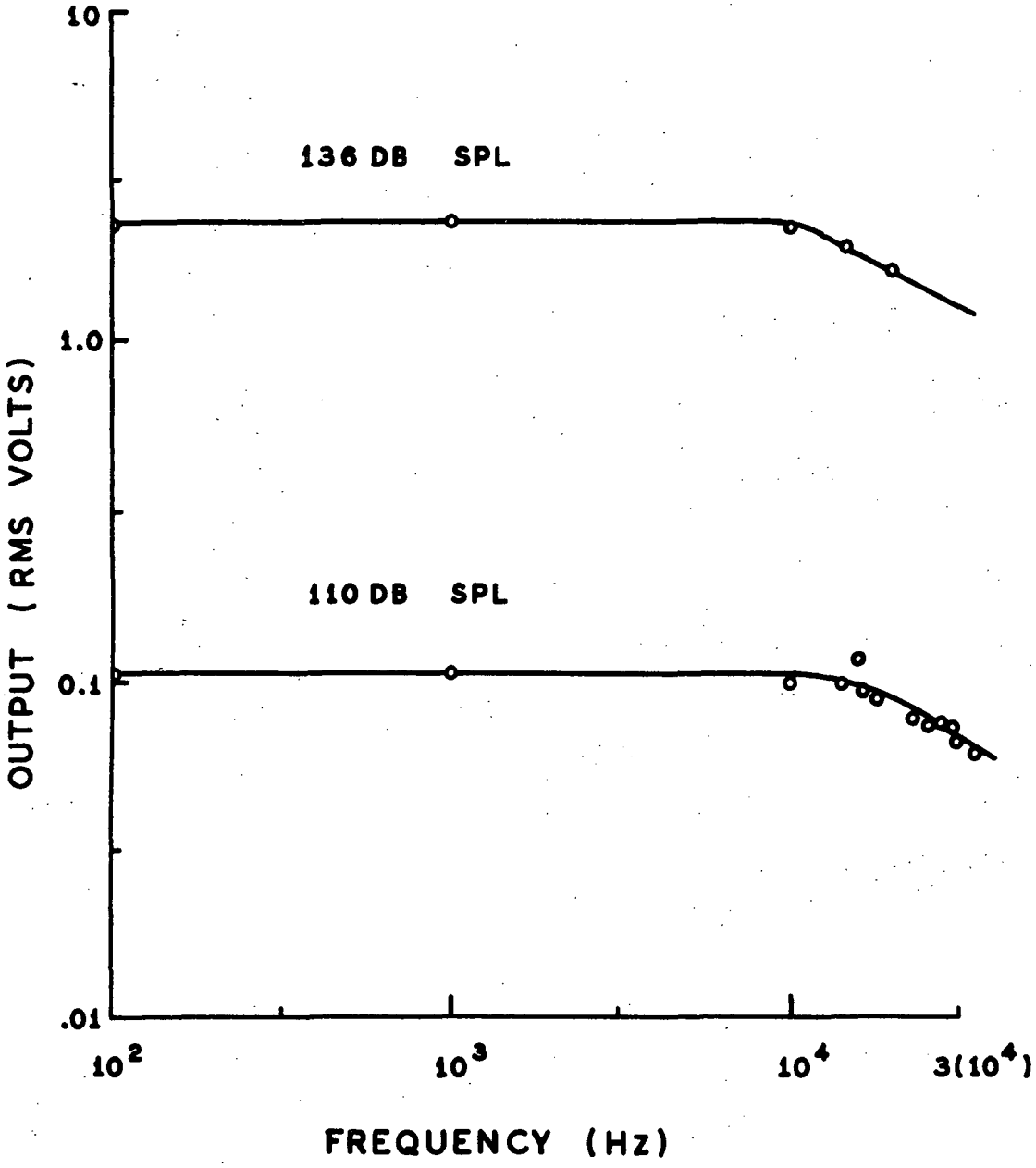

Fig. 14. Frequency response of Converter 2 at two different sound pressure levels. In both cases the cutoff frequency (-3 dB point) lies at 28 kHz.

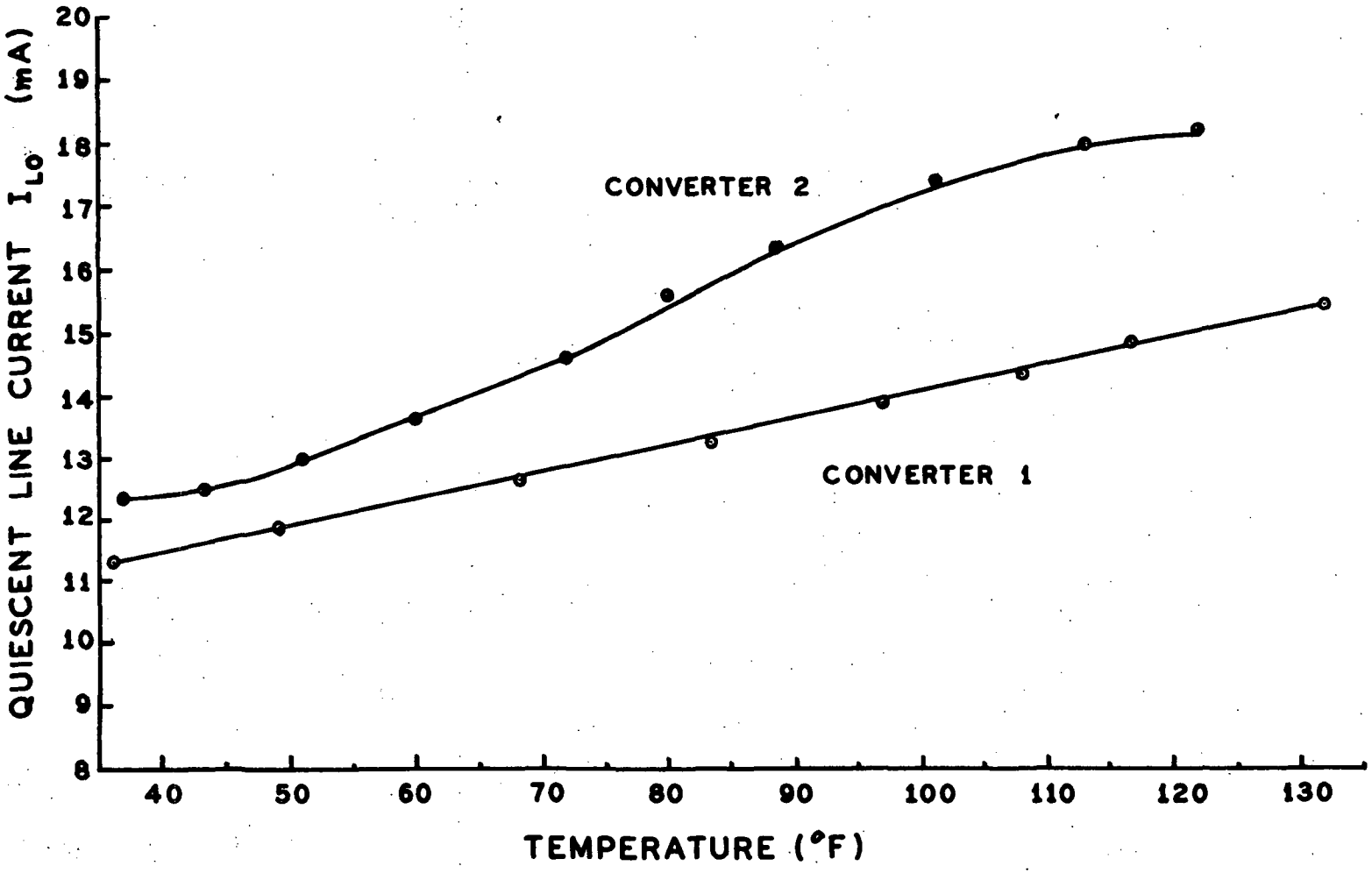

Fig. 15. Temperature dependence of converter quiescent line current. No temperature compensation is built into the converter.

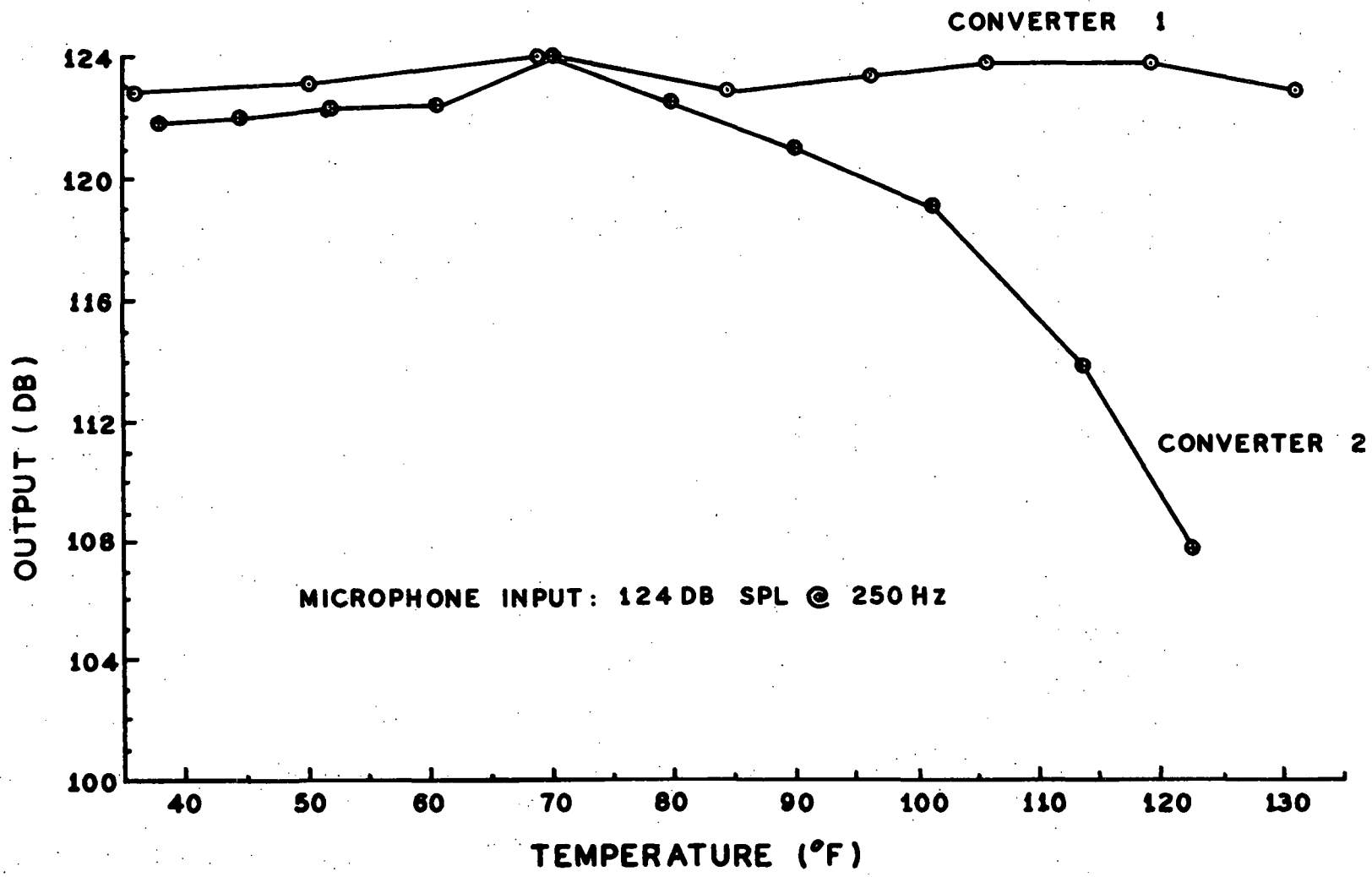

Fig. 16. Temperature dependence of converter output for a constant input at the microphone.

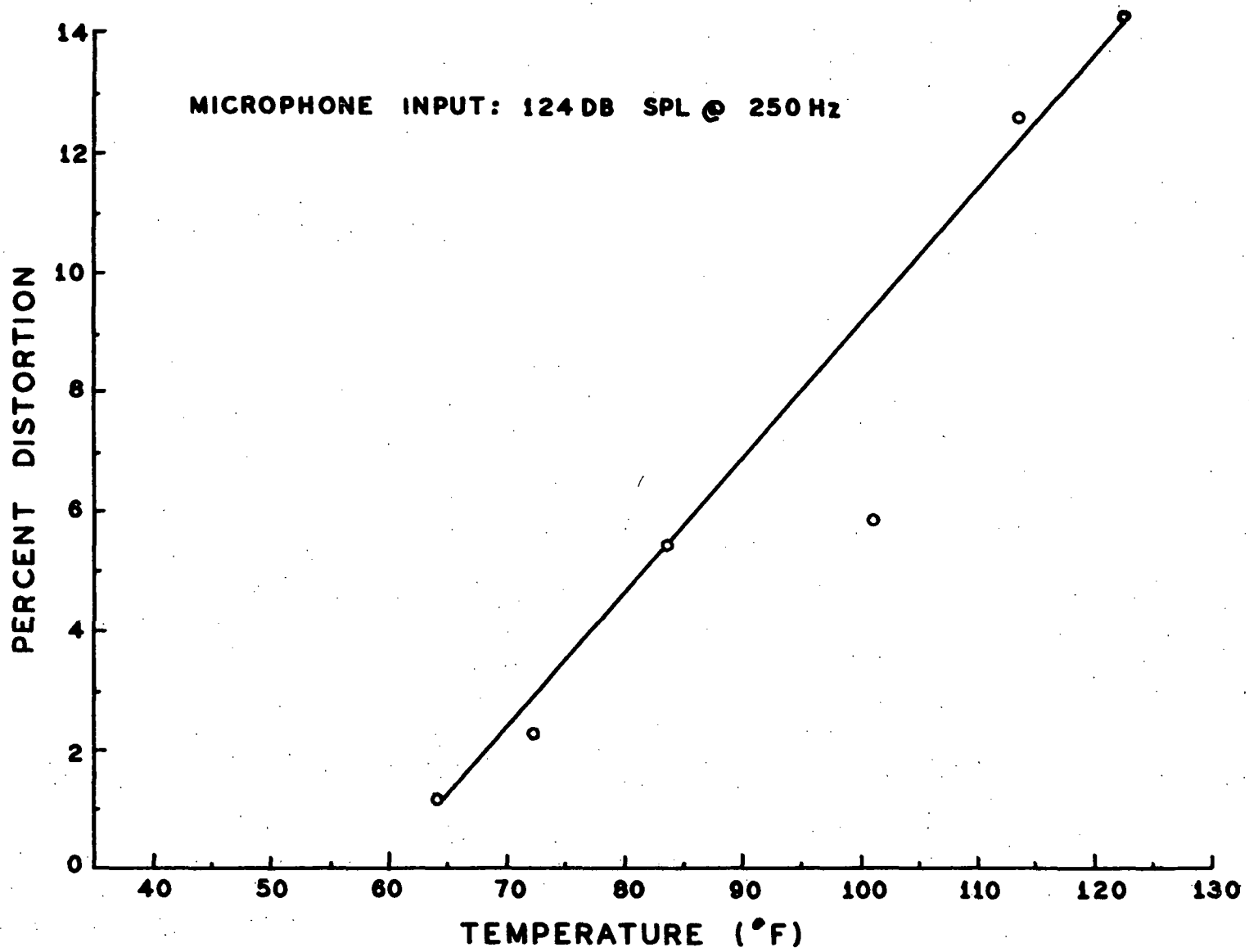

Fig. 17. Temperature dependence of the distortion of Converter 2.

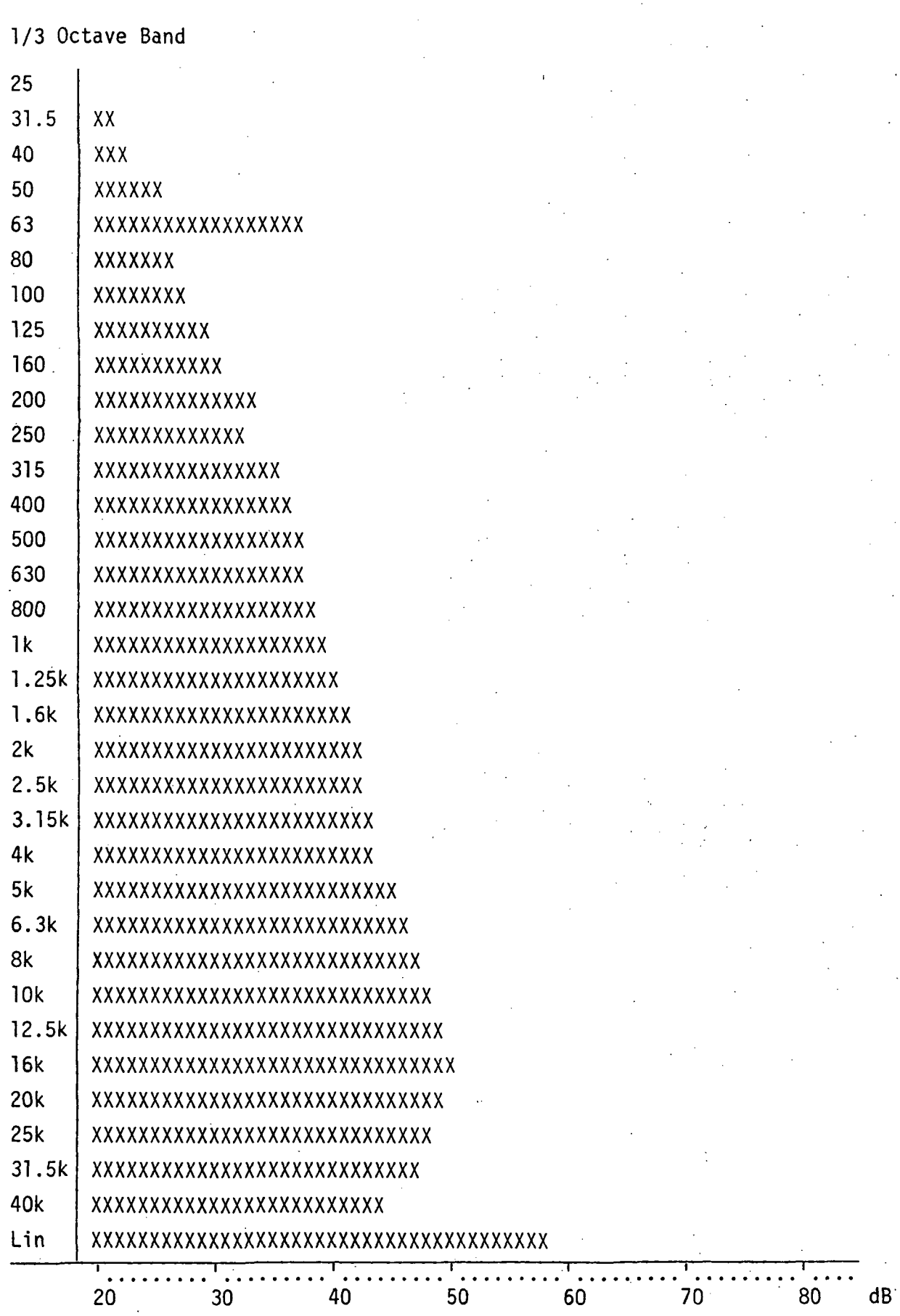

Fig. 18. Noise spectrum of General Radio 1" system (sound level meter set to 100 dB).

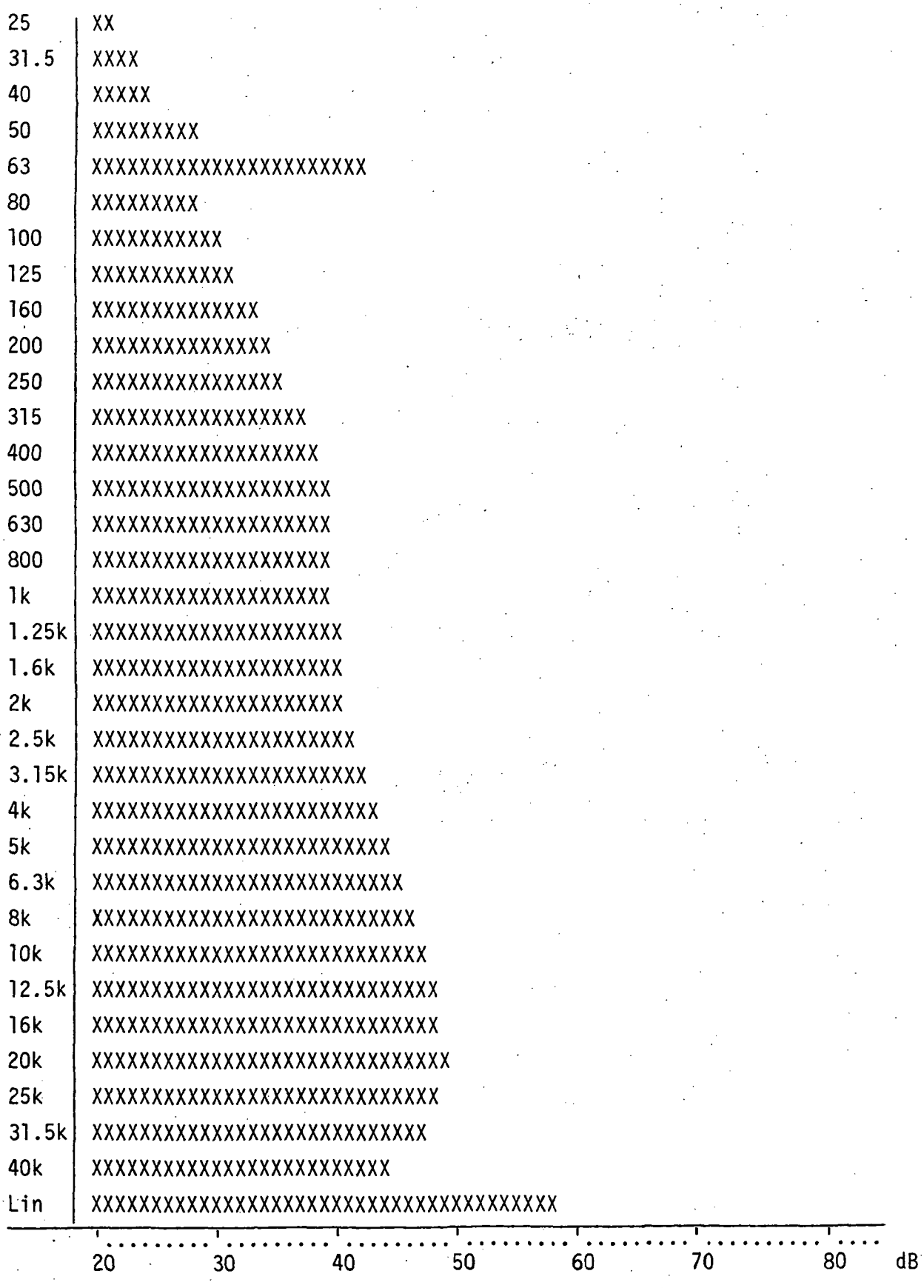

Fig. 19. Noise spectrum of General Radio 1/2" system (sound level meter set to 100 dB).

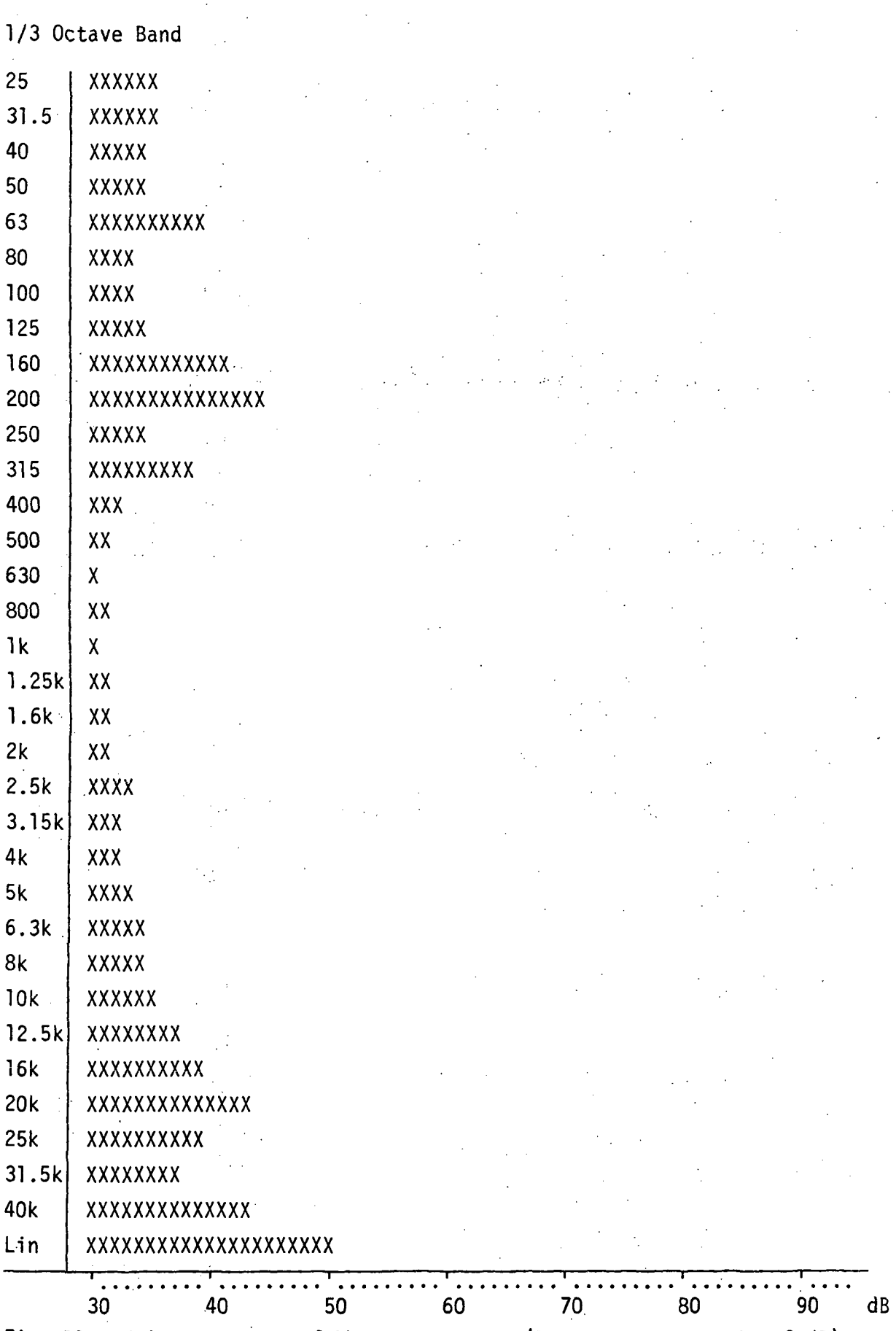

Fig. 20. Noise spectrum of Photocon system (Dynagage attenuation 0 dB).

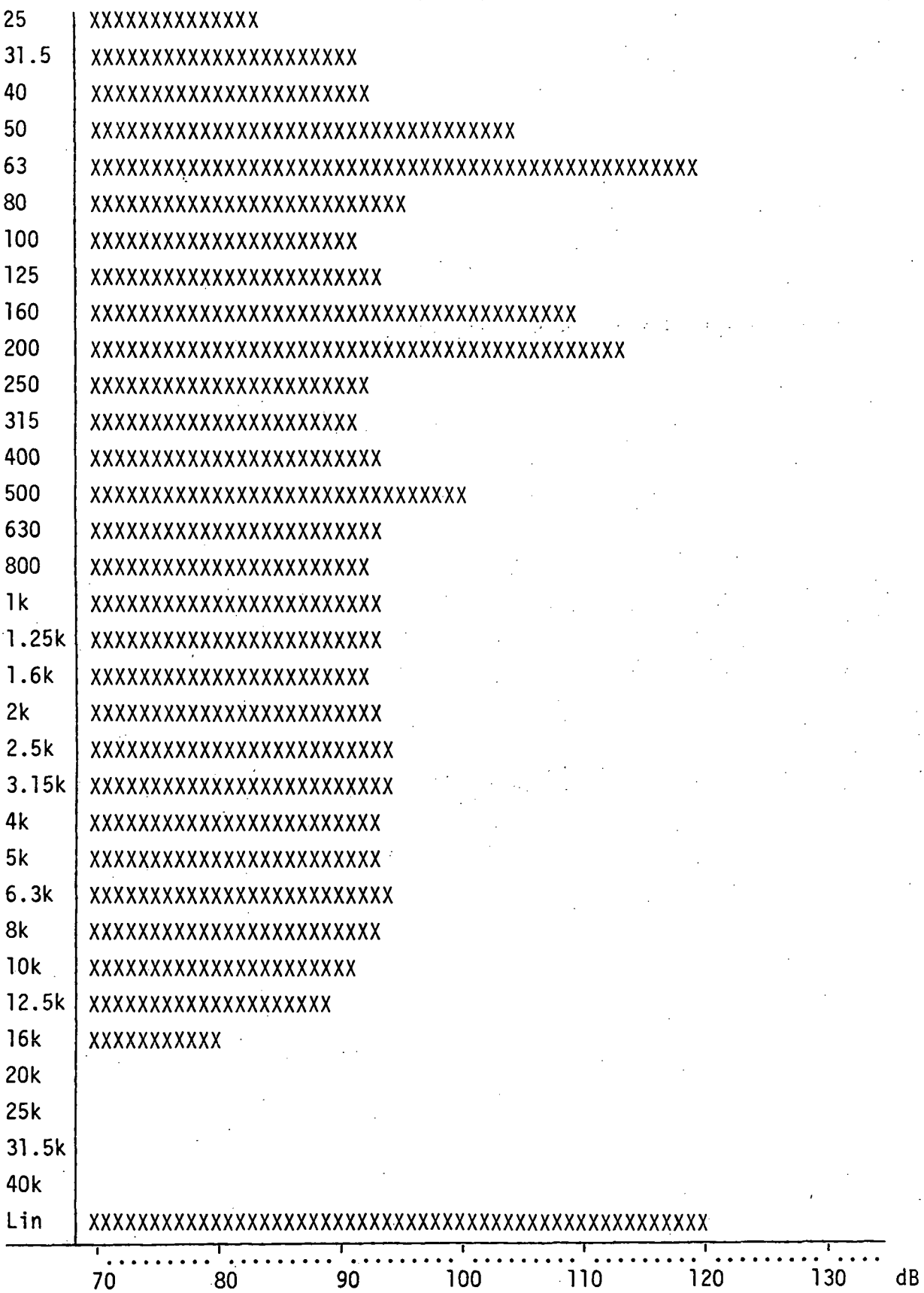

Fig. 21a. Noise spectrum of GR 1/2" system over 1000' cable during the field test of Aug. 2, 1972. A dummy microphone was connected to the preamplifier.

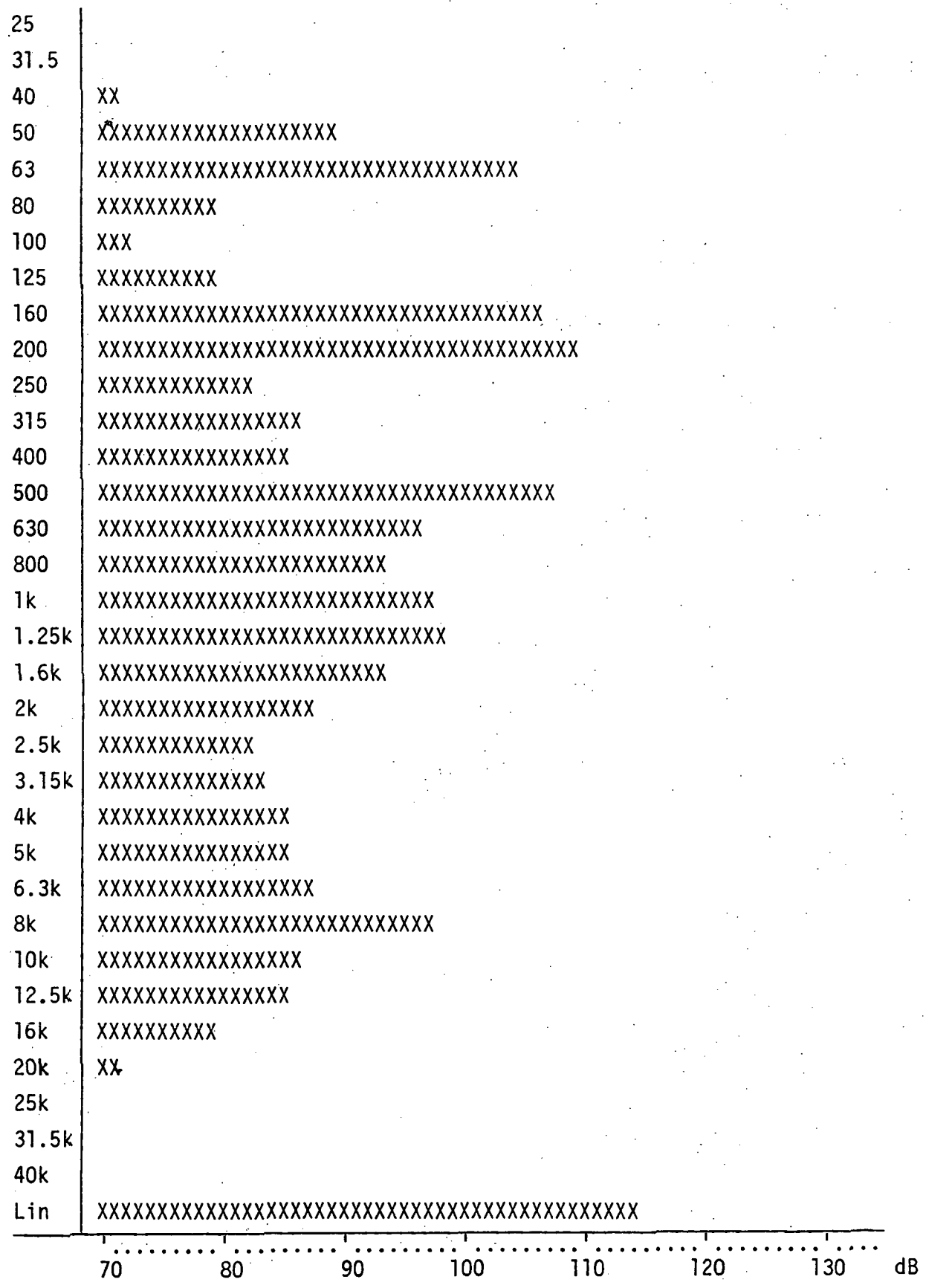

Fig. 21b. Noise spectrum of Converter 2-N400 System over 1000' cable during field test of Aug. 2, 1972. A dummy microphone was connected to the converter.

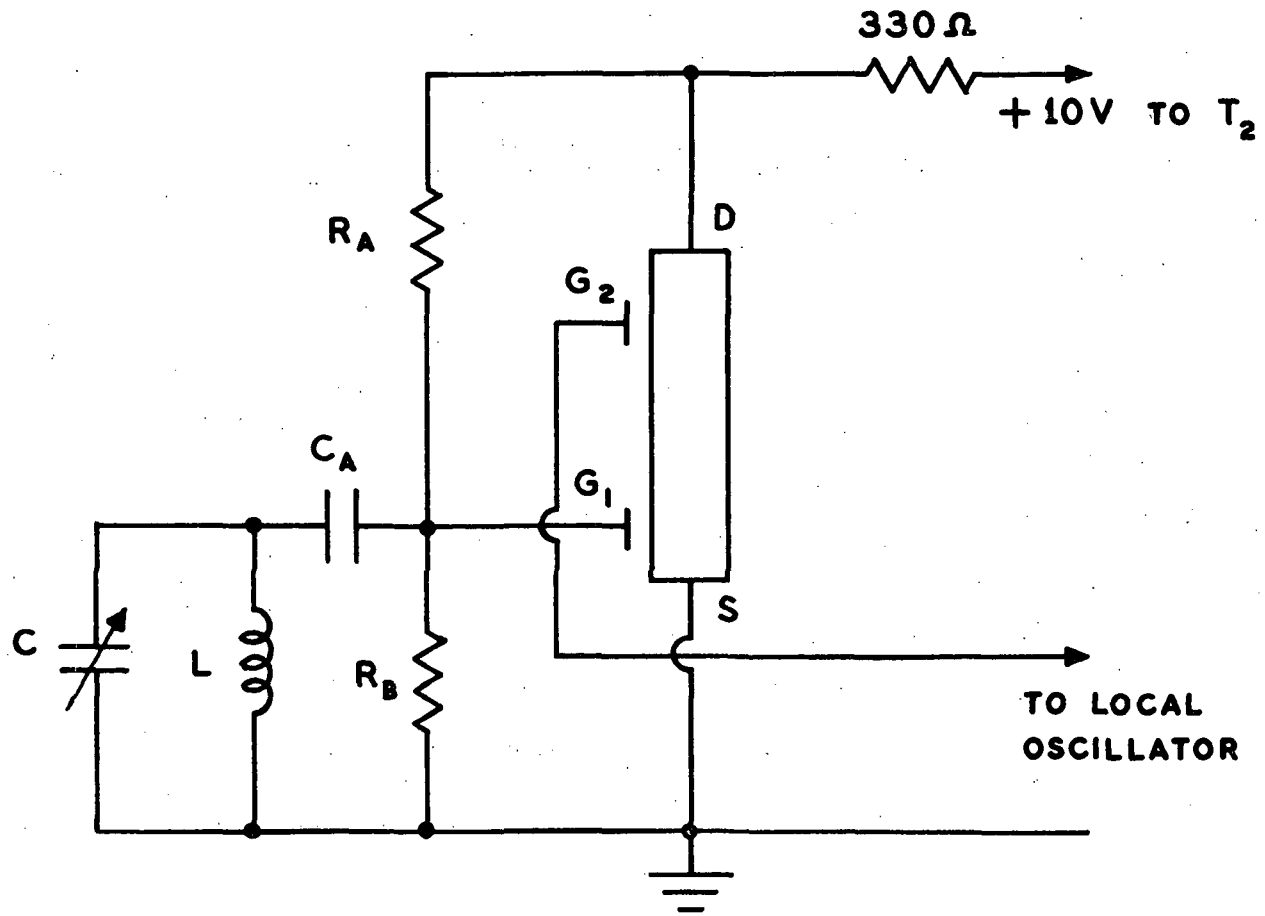

Fig. 22. Proposed network for improving the temperature stability of the converter.

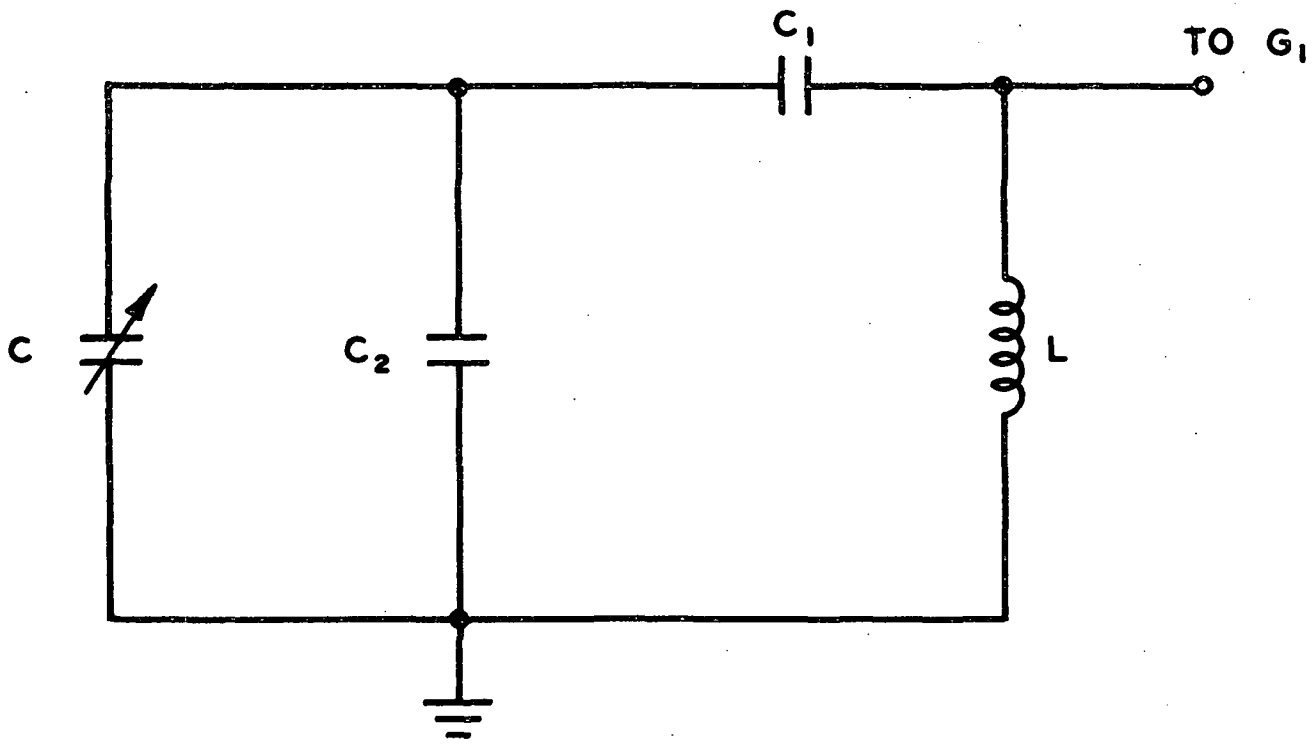

Fig. 23. Proposed network for reducing converter sensitivity.

1. Report No.	2. Government Accession No.	3. Recipient's Catalog No.
4. Title and Subtitle A SOLID STATE CONVERTER FOR MEASUREMENT OF AIRCRAFT NOISE AND SONIC BOOM		5. Report Date 6. Performing Organization Code
7. Author(s) Allan J. Zuckerwar		8. Performing Organization Report No.
9. Performing Organization Name and Address Youngstown State University Youngstown, Ohio 44503		10. Work Unit No. 501-04-01-02 11. Contract or Grant No. NGR-36-028-004
12. Sponsoring Agency Name and Address		13. Type of Report and Period Covered 14. Sponsoring Agency Code

15. Supplementary Notes

16. Abstract

The problems inherent in present systems of instrumentation for measuring aircraft noise and sonic boom include limited frequency response, expensive connecting cables, sensitivity to cable length and type, high sensitivity to environmental conditions, and additional limitations of individual system components. Furthermore, differing requirements have resulted in the use of two different systems for aircraft noise and sonic boom measurements respectively. To alleviate these difficulties a unified system of instrumentation suitable for both types of measurements has been developed. The system features a new solid state converter connected to a zero drive* amplifier. The system has been found insensitive to cable length and type up to at least 1000 ft and requires no impedance matching networks. The converter itself has a flat frequency response from dc - 28 kHz (- 3 dB), dynamic range of 72 dB, and noise floor of 50 dB in the band 22.4 Hz - 22.4 kHz.

*TM - Patent Pending, MB Electronics, Inc.

17. Key Words (Suggested by Author(s))	18. Distribution Statement
Microphone converter-acoustic measurements- Aircraft noise measurements- Infrasonic measurements	Unclassified - Unlimited

19. Security Classif. (of this report)	20. Security Classif. (of this page)	21. No. of Pages	22. Price*
Unclassified	Unclassified		